Inorganic Chemistry

Article

pubs.acs.org/IC

New Ruthenium Bis(terpyridine) Methanofullerene and Pyrrolidinofullerene Complexes: Synthesis and Electrochemical and Photophysical Properties

Kevin Barthelmes,[†,‡,⊥] Joachim Kübel,[§,∥,⊥] Andreas Winter,[†,‡] Maria Wächtler,[§,∥] Christian Friebe,[†,‡] Benjamin Dietzek,*[,‡,§,∥] and Ulrich S. Schubert*[,†,‡]

[†]Laboratory of Organic and Macromolecular Chemistry (IOMC), Friedrich Schiller University Jena, Humboldtstraße 10, 07743 Jena, Germany

[‡]Jena Center for Soft Matter (JCSM), Friedrich Schiller University Jena, Philosophenweg 7, 07743 Jena, Germany

[§]Institute of Physical Chemistry (IPC) and Abbe Center of Photonics, Friedrich Schiller University Jena, Helmholtzweg 4, 07743 Jena, Germany

[∥]Leibniz Institute of Photonic Technology e.V. (IPHT), Albert-Einstein-Straße 9, 07745 Jena, Germany

Supporting Information

ABSTRACT: A series of terpyridine (tpy) methanofullerene and pyrrolidinofullerene dyads linked via *p*-phenylene or *p*-phenyleneethynylenephenylene (PEP) units is presented. The coordination to ruthenium(II) yields donor−bridge−acceptor assemblies with different lengths. Cyclic voltammetry and UV−vis and luminescence spectroscopy are applied to study the electronic interactions between the active moieties. It is shown that, upon light excitation of the ruthenium(II)-based ^{1}MLCT transition, the formed ^{3}MLCT state is readily quenched in the presence of C_{60}. The photoinduced dynamics have been studied by transient absorption spectroscopy, which reveals fast depopulation of the ^{3}MLCT (73−406 ps). As a consequence, energy transfer occurs, populating a long-lived triplet state, which could be assigned to the $^3C_{60}$* state.

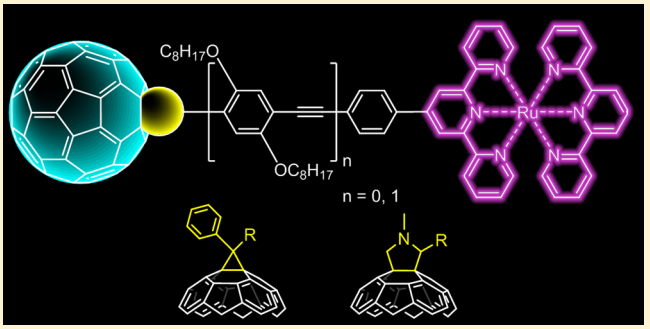

INTRODUCTION

The development of artificial devices that mimic light-triggered reactions in natural photosynthetic systems, which are based on the fundamental processes of energy and/or electron transfer, has become an attractive field in modern science and technology.[1−10] A general challenge in the molecular design of donor−bridge−acceptor systems is the generation of long-lived charge-separated (CS) states.[8,11,12] Fullerenes, in particular C_{60}, have high electron affinities, which make them favorable systems regarding their electron-accepting ability. Photoinduced electron transfer and energy transfer in (macro)-molecular assemblies containing donors, such as ferrocene,[13,14] porphyrin,[15] tetrathiafulvalene,[16,17] and others,[18,19] which are covalently linked to fullerene, were extensively studied; their electrochemical and photophysical properties are of particular interest.[20,21] Ruthenium(II) polypyridyl complexes as donors are promising materials due to their intense light absorption in the visible range and extended excited-state lifetimes.[22−24] Previous studies on Ru(II)−polypyridine−C_{60} assemblies showed that both electron and energy transfer is possible in such systems: the intermediate CS state may undergo charge recombination to the final lower lying triplet excited $^3C_{60}$* state.[25−30] Furthermore, the linker plays a crucial role in the electronic communication between the donor and acceptor parts. Several wirelike bridging units have been studied in recent years, including π-conjugated oligomers consisting of phenyleneethynylenes,[16,26] phenylenevinylenes,[31] and fluorene units[13,17] and nonconjugated oligomers consisting of glycol,[32,33] cyclohexane,[28] and peptide units.[34]

In this work, we report the investigation of new donor−acceptor systems, in which Ru(II) bis(terpyridine) complexes are connected to C_{60}. The series contains short phenyl-bridged as well as longer octyloxy-substituted phenyleneethynylenephenylene-bridged systems (Figure 1). These were chosen for their rigidity and π conjugation with low attenuation factors β,[35] which provide pathways for an efficient charge transport. Photophysical studies of these bridging units, especially in ruthenium(II) bis(terpyridine) complexes, have been thoroughly described by us previously.[36−39] This latter concept was further extended for the functionalization on C_{60} by cycloaddition reactions of 1,3-dipolar reagents with one [6,6]-double bond to form pyrrolidine or cyclopropane monoadducts. Martín and co-workers could show that cyclopropane adducts

Received: October 7, 2014
Published: March 12, 2015

DOI: 10.1021/ic502431x
Inorg. Chem. 2015, 54, 3159−3171

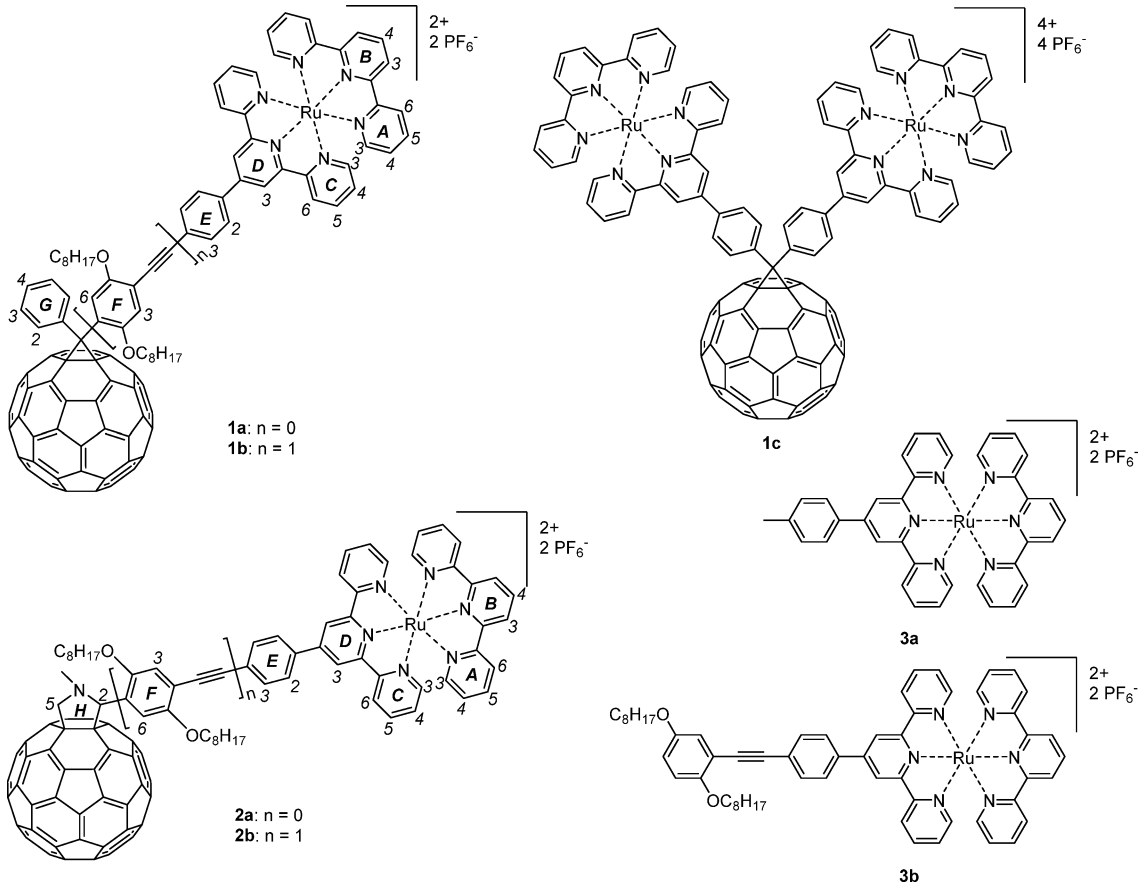

Figure 1. Schematic representations of the Ru(II)−bis(terpyridine)−C_{60} assemblies **1** and **2** as well as reference compounds **3** studied in this work, along with a numbering scheme for the complexes and precursors.

Scheme 1. Schematic Representation of the Synthetic Route[a]

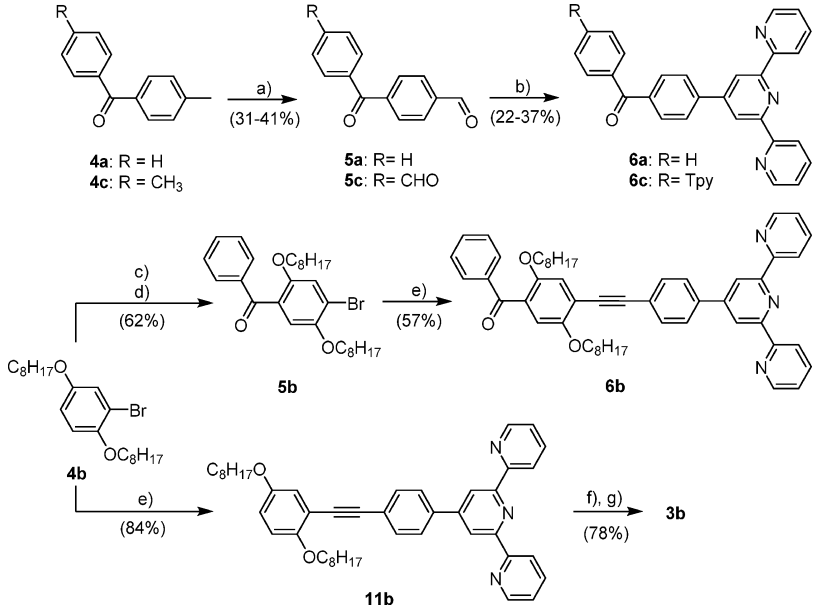

[a]Legend: (a) CrO_3, H_2SO_4, acetic anhydride, room temperature, 16 h; (b) (i) 2-acetylpyridine, NaOH, grinding, room temperature, 30 min, (ii) ammonia (aqueous), EtOH, room temperature, 48 h; (c) benzoyl chloride, $AlCl_3$, dichloromethane, room temperature, 16 h; (d) 1-bromooctane, KOH, DMSO, room temperature, 22 h; (e) 4′-(4-ethynylphenyl)-2,2′:6′,2″-terpyridine, $[Pd(PPh_3)_4]$, CuI, NEt_3, THF, 60 °C, 48−72 h; (f) $[Ru(tpy)Cl_3]$, $AgBF_4$, acetone, 70 °C, 2 h; (g) (i) DMF, 160 °C, 3 h, (ii) excess NH_4PF_6.

generally enhance the electronic communication between fluorene and C_{60} in comparison to pyrrolidine rings.[40] In addition to the mononuclear complexes **1a**,**b** and **2a**,**b**, we report the symmetrical dinuclear complex **1c**, bearing two

DOI: 10.1021/ic502431x
Inorg. Chem. 2015, 54, 3159−3171

Scheme 2. Schematic Representation of the Synthetic Route toward the Studied Ru(II) Complexes 1a−c and 2a,b[a]

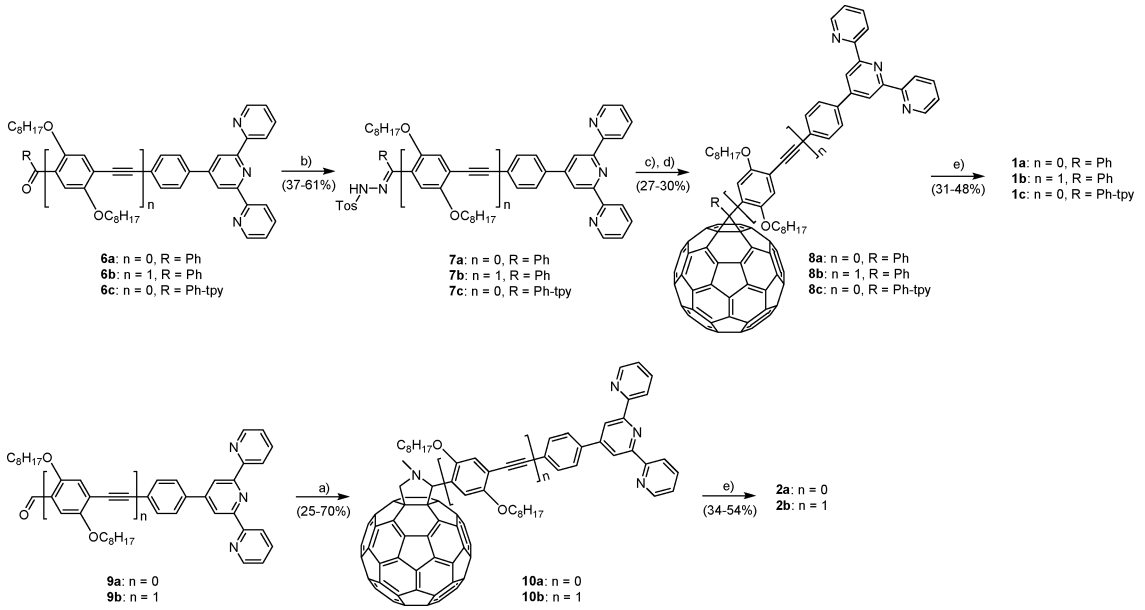

[a]Legend: (a) C_{60}, *N*-methylglycine, toluene, 120 °C, 24 h; (b) tosylhydrazine, tosylic acid, THF, 80 °C, 2−5 days; (c) $NaOCH_3$, pyridine, room temperature, 20 min; (d) C_{60}, *o*-dichlorobenzene, 180 °C, 24 h; (e) $[Ru(tpy)(MeCN)_3](PF_6)_2$, DMF, 140 °C, microwave, 30 min.

Table 1. Electrochemical Data Obtained by Cyclic Voltammetry[a]

	$E_{1/2,ox}$(Ru and/or irr P)/V	$E_{1/2,red}$(C_{60},1)/V	$E_{1/2,red}$(C_{60},2)/V	$E_{1/2,red}$(tpy,1)/V	$E_{1/2,red}$(C_{60},3 and/or tpy,2)/V
C_{60}[b]		−1.00	−1.39		−1.86
8a		−1.11	−1.49		−1.98
8b		−1.14	−1.52		−2.02
8c		−1.11	−1.48		−1.98
10a	+0.99[c]	−1.15	−1.51		−2.03
10b	+0.92[c]	−1.13	−1.53		*e*
1a	+0.91	−1.09	−1.45	−1.68	*e*
1b	+0.89	−1.12	−1.49	−1.65	*e*
1c	+0.92	−1.08	−1.46	−1.66	*e*
2a	+0.90[d]	−1.11	−1.50	−1.65	*e*
2b	+0.90[d]	−1.14	−1.50	−1.63	*e*
3a	+0.91			−1.63	−1.95
3b	+0.89			−1.59	−1.95

[a]Conditions: potentials referenced to Fc^+/Fc; scan rate 200 mV s^{-1}; glassy-carbon-disk working electrode; AgCl/Ag reference electrode; Pt-rod counter electrode; 0.1 M Bu_4NPF_6 in dichloromethane. [b]Taken from ref 68. [c]Irreversible process. The peak potential is shown. [d]Two processes. [e]Not detectable.

bis(terpyridine) ruthenium(II) centers and one C_{60} unit. The major aim of these studies is to figure out the influence of the length of the linker as well as the way the linker is connected to the C_{60} on the electrochemical and photophysical properties of the new compounds.

RESULTS AND DISCUSSION

Synthesis. The synthetic routes are depicted in Schemes 1 and 2. The benzophenone building blocks with rigid phenyl units as spacers were synthesized in a two-step reaction. Starting from para-substituted methylbenzophenones **4a,c**, the oxidation with chromium(VI) oxide yielded the desired mono- and bis-formylated[41] compounds **5a,c**, respectively. The terpyridine fragments **6a** and **6c** were prepared according to a modified Kröhnke-type procedure reported previously.[42] By grinding the starting material **5a** or **5c**, 2-acetylpyridine, and NaOH, the diketone intermediate can be prepared under these solvent-free conditions in 30 min. When the bridge length was increased, octyloxy chains were introduced to improve the solubility. For this purpose, the starting material **4b** was synthesized according to literature procedures.[43] Compound **5b** was prepared by Friedel−Crafts acylation with benzoyl chloride (during the reaction, one octyl group was cleaved off and reintroduced by alkylation). A Sonogashira cross-coupling reaction with 4′-(4-ethynylphenyl)-2,2′:6′,2″-terpyridine was applied to prepare **6b**.[44] The reference ligand **11b** was synthesized in good yield by an analogous route. The respective methanofullerenes **8a,b** as well as the symmetrical bis-(terpyridine)−C_{60} compound **8c** were obtained in a three-step reaction. First, the terpyridine-functionalized benzophenones **6a−c** were reacted with tosylhydrazine and catalytic amounts of tosylic acid to yield the desired tosyl hydrazone derivatives **7a−c**. Elimination of the tosyl group with sodium methoxide by a mechanism analogous to the Bamford−Stevens

DOI: 10.1021/ic502431x
Inorg. Chem. 2015, 54, 3159−3171

reaction yielded in situ the 1,3-dipolar diazo compounds, which reacted with C_{60} to form pyrazolinofullerene derivates as intermediates.[45,46] Further thermal treatment eliminated molecular nitrogen, and the desired methanofullerenes were obtained in low to moderate yields. Recently, we reported the synthesis of the aldehyde-functionalized 2,2′:6′,2″-terpyridines **9a**,**b** used in this study.[47,48] Pyrrolidinofullerenes **10a**,**b** were synthesized by the 1,3-dipolar cycloaddition of azomethine ylides, derived from **9a**,**b**, respectively, and *N*-methylglycine to C_{60} in an optimized 1:10:4 ratio.[49] The compounds were obtained in low to good yields, respectively, mainly due to the enhanced solubility of **9b**. All fullerene ligands were purified by column chromatography using neutral alumina and *n*-hexane/toluene mixtures to remove and recover the unreacted C_{60}. $[Ru(tpy)(MeCN)_3](PF_6)_2$ was used as a precursor to obtain the corresponding heteroleptic ruthenium(II) complexes **1a**−**c** and **2a**,**b** in moderate yields. The reaction was performed under microwave irradiation for 30 min at 140 °C in DMF. Since column chromatography using silica with potassium nitrate was not applicable for these C_{60}-containing complexes, the dark red complexes were purified by treatment of a concentrated acetonitrile solution with diethyl ether vapor to force slow precipitation. So far, we have not been able to obtain single crystals suitable for X-ray structure analysis. The reference ligands 4′-(4-methylphenyl)-2,2′:6′,2″-terpyridine (ttpy) and **11b** were coordinated to ruthenium by standard complexation procedures in ethanol[50,51] or DMF.[52] All complexes exhibited a good solubility in polar solvents, such as acetonitrile, and have been characterized by NMR spectroscopy, mass spectrometry, and elemental analysis.

Electrochemical Properties. The redox behavior of the complexes **1a**−**c** and **2a**,**b**, the ligands **8a**−**c** and **10a**,**b**, and the references **3a**,**b** was studied by cyclic voltammetry. The data are summarized in Table 1, and representative spectra are depicted in Figure 2. The electrochemical measurements were performed in dichloromethane at room temperature with Bu_4NPF_6 as the conducting salt. For complexes **1a**−**c** and **2a**,**b**, the first oxidation wave at ca. 0.9 V arises from the reversible Ru(III)/Ru(II) redox couple. In addition, for the ligands **10a**,**b**, a second, irreversible oxidation, which is overlaid by the ruthenium oxidation in **2a**,**b**, was observed. This process is attributed to the electrochemical retrocycloaddition of the pyrrolidinofullerene fragment.[53] There is no significant difference for the Ru(III)/Ru(II) redox potentials within the series (and also in comparison to the reference complexes **3a**,**b**), indicating the negligible influence of the ligand sphere on the energy of the highest occupied molecular orbital. Within the accessible potential window, all fullerene-containing compounds of the series feature three reversible C_{60}-based reduction waves of similar redox potentials at around −1.1, −1.5, and −2.0 V. The half-wave potentials are shifted cathodically in comparison to pristine C_{60}. This can be attributed to the attached pyrrolidine and cyclopropane units, causing a disruption of π conjugation and a decreased electron affinity of C_{60}.[54] As reported elsewhere,[40] the values for the C_{60} reductions are slightly cathodically shifted (around 20 mV) on comparison of pyrrolidine to cyclopropane rings attached to C_{60}. Accordingly, electron delocalization is more efficient in the methanofullerene compounds. Another trend that holds true—at least for the first C_{60}-based reduction—is the cathodic shift on changing to larger bridge lengths. The third reduction wave at around −1.65 V of **1a**−**c** and **2a**,**b** is attributed to the first reduction of the terpyridine unit. The assignment is proven by comparison of the dinuclear complex **1c** to the parent mononuclear ruthenium complex **1a**. Apparently, the dinuclear complex shows similar values for the half-wave potentials but increased currents for the ruthenium- and terpyridine-related redox couples, while the C_{60}-based peak currents stay nearly constant (see Figure S3 in the Supporting Information). The second reduction of the terpyridine unit is in the same range as the third C_{60}-based reduction. According to the model complexes **3a**,**b**, the redox potential of the second terpyridine reduction is at ca. −1.95 V (see Figure S2 in the Supporting Information). In the methanofullerene ruthenium(II) complexes **1a**−**c** there is another irreversible process around −1.98 V (see Figure S4 in the Supporting Information). As is known from the literature, this process has to be assigned to the electrochemical retrocycloaddition of Bingel adducts.[55] However, this process can only be observed for the investigated complexes and is absent for the ligands **8a**−**c**.

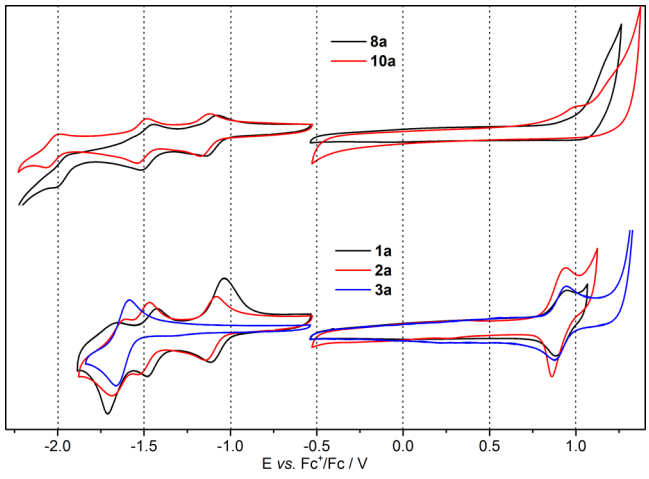

Figure 2. Cyclic voltammograms of phenyl-bridged methano- and pyrrolidinofullerene ligands and complexes in dichloromethane (with 0.1 M Bu_4NPF_6).

Photophysical Properties. The UV−vis absorption data are summarized in Table 2. A comparison of the UV−vis absorption spectra of C_{60}, **2b**, and **3b**, as shown in Figure 3, reveals that the spectrum of **2b** can be regarded as a superposition of the spectra of C_{60} and **3b**. In agreement

Table 2. UV−Vis Absorption Data[a]

	λ_{abs}/nm (ε/10^3 M^{-1} cm^{-1})[b]
C_{60}	405 (2.7), 329 (50.9), 258 (189.6)
8a	430 (2.6), 327 (46.0), 259 (150.0)
8b	430 (4.0), 328 (78.2), 259 (157.5)
8c	430 (3.1), 323 (61.4), 276 (sh, 172.9), 259 (195.5)
10a	430 (6.2), 317 (sh, 45.0), 271 (sh, 107.0), 256 (123.8)
10b	430 (10.3), 311 (87.4), 269 (sh, 126.5) 255 (149.0)
1a	484 (25.1), 327 (sh, 78.1), 310 (97.7), 270 (112.6)
1b	487 (31.6), 327 (sh, 83.9), 311 (107.2), 273 (105.4)
1c	484 (47.0), 326 (sh, 131.5), 310 (174.5), 273 (159.7)
2a	485 (22.8), 327 (sh, 59.3), 309 (83.7), 273 (85.8)
2b	488 (35.8), 327 (sh, 95.0), 311 (116.8), 270 (113.9)
3a	484 (23.4), 327 (sh, 43.4), 309 (77.5), 274 (49.3)
3b	487 (35.4), 326 (69.2), 310 (95.6), 274 (52.3)

[a]Measured in dichloromethane at 20 °C. [b]sh = shoulder.

DOI: 10.1021/ic502431x
Inorg. Chem. 2015, 54, 3159−3171

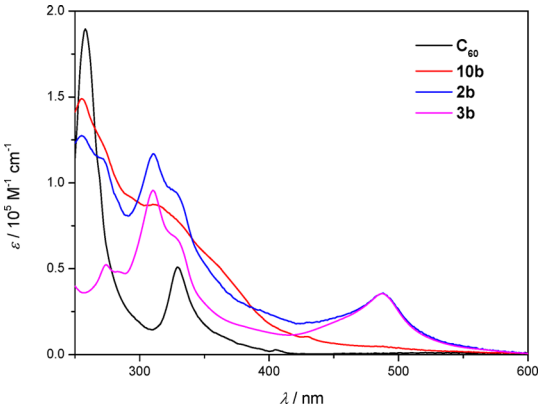

Figure 3. UV−vis absorption spectra of the long bridged pyrrolidinofullerene ligand and complexes measured in dichloromethane.

with the electrochemical measurements, there is no evidence for an electronic interaction between the Ru(II) center and the fullerene unit in the ground state. The spectral properties are similar throughout the series: while intense absorption bands between 250 and 350 nm are based on $\pi-\pi^*$ transitions within the fullerene, phenyl, and terpyridine groups, absorption bands in the region around 485 nm are related to Ru(II)-based metal-to-ligand charge-transfer (MLCT) transitions.[56] With an increased bridge length in compounds **1b** and **2b**, the additional phenylene and ethynylene groups cause a slight bathochromic shift of the $\pi-\pi^*$ transitions. An analogous behavior is observed for the MLCT transition (shift of around 3 nm), in concert with increases in the molar extinction coefficients. The fullerene ligands **8a−c** and **10a,b** possess a sharp absorption band at around 430 nm, which is bathochromically shifted in comparison to pristine C_{60} (405 nm). This transition is characteristic of closed-[6,6] fullerene monoadducts.[57,58] In the complexes, this transition is only weakly defined, because it is overlaid by the tail of the strong MLCT transition. The emission properties of **8a−c** and **10a,b** were studied in dichloromethane and compared to the reference systems ttpy and **11b**. Upon excitation of the $\pi-\pi^*$ transition (λ_{ex} = 315 or 325 nm), there is a strong quenching of the spacer- and terpyridine-based fluorescence by a factor of ca. 200 when the C_{60} unit is attached (for details, see the Supporting Information). Additionally, the fullerene-based fluorescence at ca. 700 nm is only weakly pronounced.[13] The initially weak Ru(II)-based emission at room temperature of the reference complexes (**3a**, λ_{max} = 627 nm; **3b**, λ_{max} = 645 nm) is almost fully quenched in complexes **1a−c** and **2a,b** (Figure 4). The quenching indicates an electronic interaction between the ^{3}MLCT state and the fullerene unit, as detailed below.

Photoinduced Dynamics. *Formation of the Long-Lived Excited State.* The photoinduced dynamics occurring after excitation of the ^{1}MLCT transition (λ_{exc} = 520 nm) were investigated using transient absorption (TA) spectroscopy in order to clarify the quenching mechanism. To provide consistency with the steady-state data, we will focus on the TA experiments performed in dichloromethane. Figure 5 contains transient absorption data for **2b** and for the C_{60}-free complex **3b**, as reference. The transient absorption spectra recorded for **3b** (Figure 5A) match those of typical Ru^{II} polypyridine complexes featuring ground-state bleach (GSB) in the region of the ^{1}MLCT absorption band and excited-state absorption (ESA) above 550 nm. The electronic delocalization of the ^{3}MLCT state over the extended ligand is apparent: the ESA maximum of **3a**, where ^{3}MLCT delocalization is limited to the ttpy ligand, is at ca. 560 nm in acetonitrile (see the Supporting Information). However, for **3b** the ESA maximum is located at ca. 690 nm, clearly indicating the presence of an extended π system.[59] This was also noted for related methoxyphenyl-substituted $[Ru(bpy)_3]^{2+}$ derivatives.[26] The kinetic traces (Figure 5B) illustrate that the signal decay is not completely resolved, at least within the time scale of the experiment. However, this decay likely corresponds to the decay of the ^{3}MLCT (see below).

The quantitative interpretation of the TA data is based on global multiexponential fits corresponding to a kinetic scheme involving consecutive first-order reactions (details are given in the Experimental Section). In the case of **3b**, four kinetic components are used to fit the data. The decay-associated spectra (DAS) and the corresponding characteristic time constants are given in Figure 6. The DAS (τ_4 = 1.6 ns) features a much higher amplitude than the other DAS: i.e., it plays a dominant role in the photoinduced dynamics of **3b**. The DAS (τ_4) reflects the shape of the TA spectra recorded at long delay times, indicating that τ_4 describes the decay of the

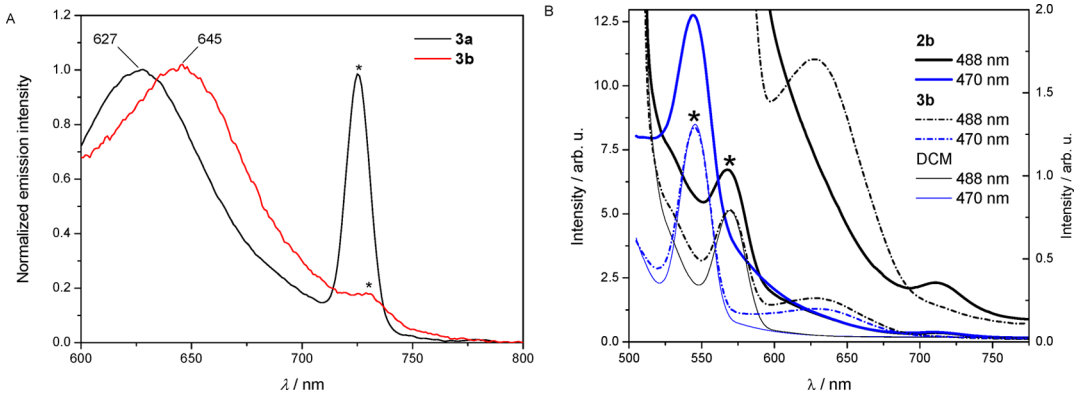

Figure 4. (A) Normalized emission spectra (λ_{ex} = 483 or 488 nm) of the reference complexes **3a,b** measured in dichloromethane at room temperature. Asterisks mark the scattered excitation light. (B) Emission spectra of isoabsorbing solutions at 487 nm of **3b** and **2b** in dichloromethane together with the signal obtained from the pure solvent. The right scale shows a magnification of the spectral region containing ^{3}MLCT phosphorescence and C_{60} fluorescence (solvent and spectra recorded at 470 nm are omitted for clarity).

DOI: 10.1021/ic502431x
Inorg. Chem. 2015, 54, 3159−3171

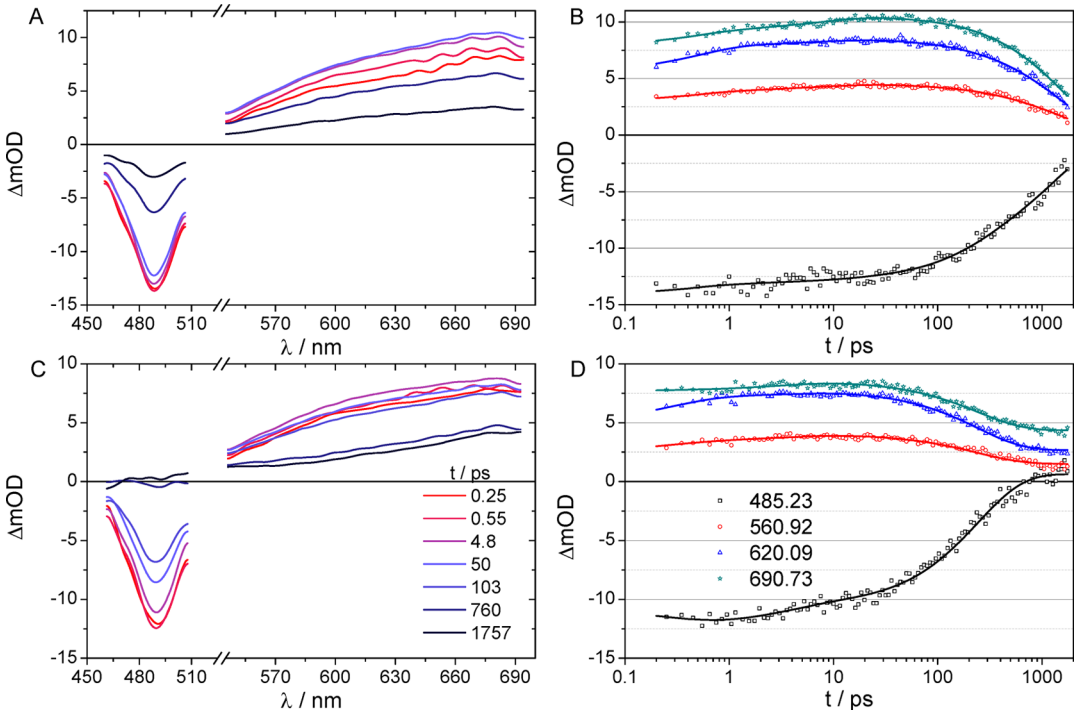

Figure 5. Transient absorption spectra (A, C) at selected delay times between 0.2 and 1.8 ns (from red to black) and selected kinetic traces (B, D) with corresponding fit curves: 488 nm (black squares), 560 nm (red circles), 620 nm (blue triangles), and 690 nm (cyan stars) for **3b** (A, B) and **2b** (C, D).

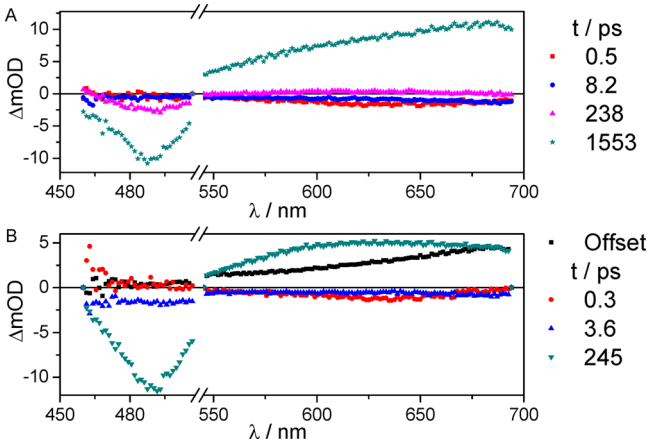

Figure 6. Global fit results in terms of decay-associated spectra for **3b** (A) and **2b** (B). The characteristic time constants are given in the legends.

^{3}MLCT and, thus, the overall decay to the ground state. This is also supported by the emission decay time of **3b** (2.3 ns in acetonitrile), determined by time-correlated single-photon counting (see the Supporting Information). This value can be compared to the 1.6 ns decay time determined in the TA experiments, as in the latter decay time there is a relatively large uncertainty due to the limited delay time range (1.8 ns) accessible in our experimental setup.

The fastest component (τ_1 = 0.5 ps) is assigned to solvent relaxation and vibrational energy dissipation[60,61] and causes an increase of the ESA between 550 and 700 nm. Generally, the picosecond components (τ_2 = 8.2 ps, τ_3 = 238 ps) can be attributed to the presence of the organic chromophore attached at the 4′-position of the tpy unit:[62] Here, the process associated with τ_2 is assigned to photoinduced planarization of the extended terpyridine ligand: i.e., excited-state torsional motion around the pyridine−phenyl bond.[63] Planarization causes an increase in the ESA in the visible part of the spectrum due to an enhanced π conjugation of the ligand. DFT calculations on **3b** suggest a strong mixing of ^{3}MLCT states with ligand-centered orbitals (see the Supporting Information) leading to delocalized states with different amounts of ^{3}MLCT and ^{3}LC character. Therefore, τ_3 (238 ps) has to be assigned to an equilibration between close-lying, mixed triplet states.[39,64]

Dyad **2b** shows transient absorption features similar to those observed for **3b** at early delay times (see Figure 5A,B). Both the spectra and the kinetic traces are similar up to 30 ps. Later, in **2b** a more pronounced decay is observed, which is not complete: i.e., the kinetic traces reach a plateau after ca. 1 ns. The transient absorption spectra at delay times >1.5 ns are positive over the entire spectral range probed in our experiment, including a rise toward 700 nm. Thus, the nanosecond dynamics of **2b** are clearly different from those of **3b**, leading to the formation of a long-lived species unique for the dyad. The global fit routine produces three kinetic components and an offset corresponding to the spectrum of the long-lived species formed. The nature of this species will be discussed in conjunction with results of nanosecond transient absorption experiments. The sub-picosecond component (τ_1 = 0.3 ps) is similar to the fastest process observed for **3b** and can be rationalized equivalently. The picosecond processes, i.e. the processes associated with τ_2 and τ_3, are accelerated in **2b** in comparison to those in **3b**. In detail, a process with τ_2 = 3.6 ps shows spectral characteristics similar to those of the equilibration process (τ_3) observed in **3b**. The time constant τ_3 = 245 ps of **2b** is identical with the value of τ_3 of **3b** (238 ps), but the corresponding DAS (τ_3) in the case of **2b** is basically identical with the DAS (τ_4) of **3b** describing the overall decay, as discussed above. Therefore, the depopulation of the ^{3}MLCT

DOI: 10.1021/ic502431x
Inorg. Chem. 2015, 54, 3159−3171

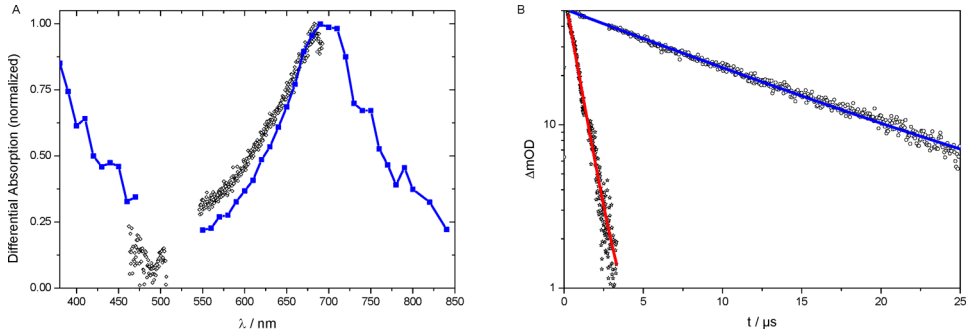

Figure 7. Nanosecond transient absorption data of **2b** in dichloromethane: (A) absorption spectra of the long-lived species constructed from integrated intervals of nanosecond transient absorption kinetics (blue solid squares) with the offset component from the femtosecond TA data (black hollow symbols) for comparison; (B) decay of the positive absorption at λ = 700 nm after photoexcitation of **2b** at 520 nm in aerated (solid stars) and deaerated (hollow spheres) solutions with respective fit curves for τ = 800 ns (red curve) and τ = 13 μs (blue curve).

(or rather a mixed ^{3}MLCT/π–π*) state occurs very quickly for **2b** with the same time constant that was assigned to excited-state equilibration in **3b**. Given the fact that the long-lived state in **2b** is due to the fullerene unit, the process that deactivates the ^{3}MLCT is the same process that populates the long-lived state (see below).

Nature of the Long-Lived Excited State. Nanosecond transient absorption experiments on **2b** (Figure 7) were conducted to detail the nature of the long-lived state: kinetic traces for the nano- to microsecond decay were recorded for selected wavelengths. From these curves, nanosecond transient absorption spectra were constructed. A broad absorption peak is found with a maximum at ca. 700 nm and steep flanks on both the high- and low-energy sides. A shoulder is observed at ca. 800 nm, and there are hints toward a rise at wavelengths shorter than 450 nm. The offset component determined from the femtosecond transient absorption data is in good agreement with the nanosecond transient absorption spectrum. Furthermore, the nanosecond spectrum coincides with the known absorption features of the $^3C_{60}$* state,[31] in particular the maximum at around 700 nm and the long-wavelength shoulder. Additional support for the assignment of the long-lived state as $^3C_{60}$* is based on oxygen-quenching experiments: Triplet states of organic molecules are prone to undergo quenching reactions with triplet oxygen, strongly reducing the excited-state lifetime.[65] From a comparison of kinetic traces of the ESA decay at 700 nm recorded in the presence and absence of oxygen (Figure 7B), it is taken that the lifetime significantly increases in the absence of oxygen, indicative of a triplet state. The lifetimes of 800 ns and 13 μs with and without oxygen, respectively, are consistent with literature reports on $^3C_{60}$*.[31]

Three possible quenching mechanisms leading to the $^3C_{60}$* state were discussed in the literature,[26] of which resonant triplet–triplet energy transfer (Förster-type) is unlikely to happen due to the weak acceptor absorption. Other possibilities are charge separation, i.e. a transport of the negative charge located on the ligand toward the fullerene after ^{1}MLCT excitation followed by a fast recombination, and Dexter-type energy transfer. The former would, however, yield a reduced C_{60} species, which would absorb in the NIR region at around 1100 nm.[31]

Solvent-polarity-dependent TA spectroscopy was performed to yield additional insight into the photoinduced processes and validate the absence of a photoinduced charge-transfer reaction. Therefore, additional TA measurements on **2b** and **3b** were performed in acetonitrile: despite the higher polarity of acetonitrile in comparison to dichloromethane, the data reveal almost identical spectral and temporal characteristics (see the Supporting Information). In particular, no significantly different time constants were found, ruling out the possibility that charge separation is contributing to the photophysics of **2b**. Similar observations are made for **2a**, i.e. the short-bridged analogue, as well as the methano-fullerene dyads **1a**,**b**, as the photoinduced dynamics probed in transient absorption experiments are rather similar for all of these compounds (see the Supporting Information). This holds true also for the dinuclear complex **1c**.

Nevertheless, the quenching kinetics are not identical for the compounds at hand. In fact, the rate constant for energy transfer measured in acetonitrile (corresponding to the process causing the ^{3}MLCT absorption characteristics to vanish) depends on both the linker type and the size of the bridge between terpyridine and fullerene moieties (see Figure 8). The

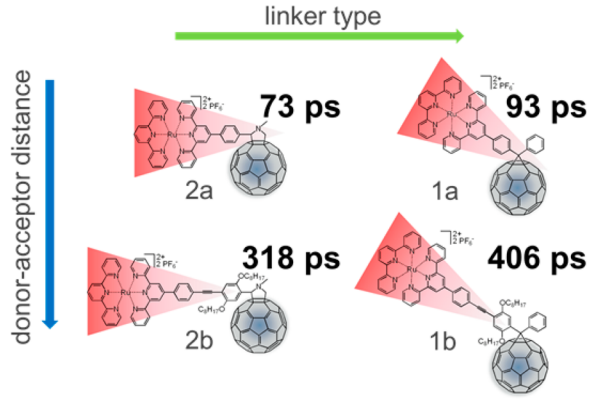

Figure 8. Schematic representation of the distance and linker dependence of the energy transfer (^{3}MLCT depopulation) rate.

fastest ^{3}MLCT deactivation (73 ps) is observed for the short-bridged pyrrolidinofullerene dyad **2a**. In **1a** the energy transfer is somewhat slower (93 ps), possibly due to the different angle of the complex fragment with respect to the fullerene surface. The larger bridge, increasing the donor–acceptor distance in the assemblies **1b** and **2b**, causes a significant prolongation of the energy transfer time.

The fact that **3b** and **2b** possess strongly delocalized ^{3}MLCT states involving orbitals of the organic chomophore indicates that orbital overlap with the fullerene unit might favor rapid Dexter-type energy transfer in the Ru(II)–C_{60} dyads. As soon as the extended ligand is planarized and electronic communi-

DOI: 10.1021/ic502431x
Inorg. Chem. 2015, 54, 3159–3171

cation between the metal center and the orbitals of the organic chromophore is enhanced, there is close spatial proximity with orbitals of the fullerene acceptor and an efficient deactivation pathway of the ^{3}MLCT is accessible.

CONCLUSION

A series of mono- and dinuclear ruthenium(II) bis(terpyridine) methanofullerene and pyrrolidinofullerene assemblies connected with phenylene and phenyleneethynylenphenylene units was synthesized. The key step of the synthetic route was the cycloaddition reaction of the terpyridine building blocks onto the fullerene unit. The complexes were compared to related reference compounds with regard to their electrochemical and photophysical properties. The methanofullerene compounds feature better electronic communication between the active units in comparison to pyrrolidinofullerenes, indicated by a small anodic shift of the C_{60}-based redox potentials. The ground-state absorption spectra are mainly a superposition of the individual moieties' characteristics, indicating weak interaction between the redox-active subunits in the ground state. However, steady-state emission spectroscopy revealed a strong interaction in the excited state: namely, by quenching of the ligand-based fluorescence and Ru(II)-based phosphorescence. Photoexcitation of the Ru(II)-based ^{1}MLCT transition results in a fast population of the lowest-lying triplet C_{60} state. A distance and linker dependence of the energy transfer rate was found. We believe that the photophysical and electrochemical properties of the presented complexes have a high potential in formation of light-induced charge-separated states for artificial photosynthetic devices, in particular when the assemblies are extended from dyads to triads by incorporation of lateral organic or organometallic donor entities. This is the topic of ongoing research.

EXPERIMENTAL SECTION

General Remarks. 2-Bromo-1,4-bis(octyloxy)benzene (**4b**),[43] 4′-(4-ethynylphenyl)-2,2′:6′,2″-terpyridine,[47] 2,5-bis(octyloxy)-4-(4-[2,2′:6′,2″]terpyridin-4′-ylphenylethynyl)benzaldehyde (**9b**),[47,48] bis-(4,4′-formyl)benzophenone (**5c**),[41] 4′-(4-formylphenyl)-2,2′:6′,2″-terpyridine (**9a**),[47] 4′-(4-methylphenyl)-2,2′:6′,2″-terpyridine (ttpy),[66] [Ru(tpy)Cl$_3$],[67] and [Ru(tpy)(MeCN)$_3$](PF$_6$)$_2$[50] were synthesized according to literature procedures. Dry toluene, THF, and dichloromethane were obtained from a Pure-Solv MD-4-EN solvent purification system (Innovative Technologies Inc.). Triethylamine was dried over KOH and distilled. All other chemicals were purchased from commercial suppliers and used as received. All reactions were performed in oven-dried flasks and were monitored by thin-layer chromatography (TLC) (silica gel on aluminum sheets with fluorescent dye F254, Merck KGaA). Microwave reactions were carried out using a Biotage Initiator Microwave synthesizer. NMR spectra were recorded on a Bruker AVANCE 250 MHz, AVANCE 300 MHz, or AVANCE 400 MHz instrument in deuterated solvents (Euriso-Top) at 25 °C. ^{1}H and ^{13}C resonances were assigned using appropriate 2D correlation spectra. Chemical shifts are reported in ppm using the solvent as internal standard. Matrix-assisted laser desorption ionization time of flight (MALDI-TOF) mass spectra were obtained using an Ultraflex III TOF/TOF mass spectrometer in reflector mode. High-resolution electrospray ionization time of flight mass spectrometry (ESI-Q-TOF MS) was performed on an ESI-(Q)-TOF-MS microTOF II (Bruker Daltonics) mass spectrometer. Melting points (mp) were determined on a Stuart SMP-3 apparatus. UV−vis absorption spectra were recorded on a PerkinElmer Lambda 750 UV/vis spectrophotometer and emission spectra on Jasco FP6500 and FP-6200 instruments, respectively. Measurements were carried out using 10^{-6} M solutions of the respective solvents (spectroscopy grade) in 1 cm quartz cuvettes at room temperature. However, some emission spectra were recorded using higher absorbances (ca. 0.2 in the maximum of the ^{1}MLCT band). Cyclic voltammetry measurements were performed on a Metrohm Autolab PGSTAT30 potentiostat with a standard three-electrode configuration using a glassy-carbon-disk working electrode, a platinum-rod auxiliary electrode, and a AgCl/Ag reference electrode; a scan rate of 200 mV s^{-1} was applied. The experiments were carried out in deaerated solvents (spectroscopy grade) containing 0.1 M Bu_4NPF_6 salt. At the end of each measurement, ferrocene was added as an internal standard.

Time-Resolved Spectroscopy. The femtosecond transient absorption measurements (λ_{exc} 520 nm) were performed on two different setups. Each setup is based on an amplified Ti:sapphire oscillator (800 nm, 1 kHz). One setup produces pulses of 35 fs at 3.5 mJ (Legend-Elite, Coherent Inc., used for measurements in acetonitrile) and the other setup 100 fs at 950 μJ (Libra, Coherent Inc., used for measurements in dichloromethane). Appropriate beam splitters split the pulses to attenuate the intensity to pump: in case of the former setup, a collinear optical-parametric amplifier (TOPAS-C, LightConversion Ltd.) with 1.35 W or, for the latter setup, a noncollinear optical-parametric amplifier (TOPASwhite, Lightconversion Ltd.) with 0.5 W. The pump pulses delayed in time with respect to the probe pulses by means of an optical delay line, and their polarization was rotated by 54.7° (magic angle) with respect to the probe beam by using a Berek compensator. For both setups white light was used as the probe, which was generated by focusing a minor fraction of the amplifier output into a sapphire plate. The probe beam is focused and recollimated using 50 cm (20 cm) spherical mirrors, while the focus of the pump beam is behind the sample in order to obtain a homogeneously excited sample volume. The pump pulse is blocked after the sample, while the probe pulse is sent to a double-stripe diode-array detection system (Pascher Instruments AB) together with the reference pulse. The pump pulse energy was typically adjusted to 1 μJ while the integrated probe intensity was a few hundred nanojoules. The sample solution (OD typically ca. 0.2 at the excitation wavelength) was kept in a 1 mm quartz cuvette. Prior to data analysis, the experimental differential absorption data was chirp corrected and afterward fitted globally.

The excited-state lifetimes were determined using a nanosecond transient absorption setup. Nanosecond pump pulses at 520 nm were delivered by a Continuum Surelite OPO Plus pumped by a Continuum Surelite Nd:YAG laser (pulse duration 5 ns; pulse to pulse repetition rate 10 Hz). A 75 W xenon arc lamp provided the probe light. Spherical concave mirrors were used to focus the probe light into the sample and to refocus the light on the entrance slit of a monochromator (Acton, Princeton Instruments). The probe light was detected by a Hamamatsu R928 photomultiplier tube mounted on a five-stage base at the monochromator exit slit, and the signal was processed by a commercially available detection system (Pascher Instruments AB). Some measurements were performed in oxygen-free solutions produced by performing several freeze−pump−thaw cycles. All measurements were performed in 1 cm fluorescence cuvettes, allowing a 90° angle between pump and probe beam.

4-Formylbenzophenone (5a). The oxidation of the terminal methyl group was performed according to a related literature procedure.[41] Concentrated sulfuric acid (6 mL, 113 mmol) was added dropwise to a stirred solution of 4-methylbenzophenone (**4a**; 3 g, 15.29 mmol) in acetic anhydride (30 mL) at 0 °C. To this was added a solution of chromium(VI) oxide (4.13 g, 41.3 mmol) in acetic anhydride (20 mL) dropwise at such a rate that the temperature did not exceed 10 °C. After all the chromium(VI) oxide was added, stirring was continued for a further 16 h at room temperature. Subsequently, the reaction mixture was added to an ice−water mixture (150 mL) and the solid was collected by filtration. Further material was extracted from the solution with diethyl ether (2 × 50 mL); the ethereal extracts were dried, and the solvent was evaporated. The combined solid products were washed with 2% aqueous sodium carbonate solution (1 × 50 mL) and then heated at reflux in ethanol/water/concentrated sulfuric acid (53 mL, 10/10/1) for 30 min. The solution was cooled to room temperature, the product was extracted with ethyl acetate (4 × 50 mL), the combined organic extracts were

DOI: 10.1021/ic502431x
Inorg. Chem. 2015, 54, 3159−3171

washed with saturated aqueous sodium hydrogen carbonate solution (2 × 50 mL) and dried with Na_2SO_4, and the solvent was evaporated to yield the crude product. Further purification was achieved by flash chromatography (silica, *n*-hexane/dichloromethane 1/3) to give a yellow solid (1 g, 4.76 mmol, 31%). Mp: 67−68 °C. ^{1}H NMR (300 MHz, $CDCl_3$, ppm): δ 10.13 (s, 1H, −C*H*O), 8.00 (d, ^3J = 8.4 Hz, 2H, H^{E3}), 7.92 (d, ^3J = 8.2 Hz, 2H, H^{E2}), 7.86−7.77 (m, 2H, H^{G2}), 7.63 (t, ^3J = 7.4 Hz, 1H, H^{G4}), 7.51 (t, ^3J = 7.5 Hz, 2H, H^{G3}). ^{13}C NMR (75 MHz, $CDCl_3$, ppm): δ 195.94, 191.75, 142.70, 138.61, 136.88, 133.26, 130.45, 130.24, 129.62, 128.67. Anal. Calcd for $C_{14}H_{10}O_2$: C, 79.98; H, 4.79. Found: C, 80.11; H, 4.87.

General Procedure for Kröhnke-Type Terpyridine Synthesis. 2-Acetylpyridine (2.2 equiv per aldehyde group), aldehyde derivate **5** (1 equiv), and sodium hydroxide (2.2 equiv per aldehyde group) were ground in a mortar until a bright yellow powder was formed (10−20 min). The solid was transferred to a flask, ethanol (10 mL) and 25% aqueous ammonia solution (5 mL) were added, and the suspension was stirred at room temperature for 48 h. The gray precipitate that formed was filtered and washed with water (15 mL) and ethanol (5 mL). The crude product was recrystallized in THF.

*4‴-[2,2′:6′,2″]Terpyridin-4′-ylbenzophenone (**6a**).* According to the general procedure for Kröhnke-type terpyridine synthesis, 2-acetylpyridine (0.38 g, 3.14 mmol), 4-formylbenzophenone (**5a**; 0.3 g, 1.427 mmol), and sodium hydroxide (0.126 g, 3.14 mmol) were reacted to yield a beige solid (217 mg, 0.525 mmol, 37%). Mp: 122 °C. ^{1}H NMR (300 MHz, $CDCl_3$, ppm): δ 8.78 (s, 2H, H^{D3}), 8.73 (d, ^3J = 4.7 Hz, 2H, H^{C6}), 8.68 (d, ^3J = 8.0 Hz, 2H, H^{C3}), 8.01 (d, ^3J = 8.4 Hz, 2H, H^{E3}), 7.94 (d, ^3J = 8.3 Hz, 2H, H^{E2}), 7.92−7.81 (m, 4H, H^{C4}, H^{G2}), 7.62 (t, ^3J = 7.4 Hz, 1H, H^{G4}), 7.52 (t, ^3J = 7.4 Hz, 2H, H^{G3}), 7.36 (ddd, ^3J = 7.3 Hz, ^3J = 4.8 Hz, ^4J = 0.9 Hz, 2H, H^{C5}). ^{13}C NMR (75 MHz, $CDCl_3$, ppm): δ 196.35, 156.27, 156.09, 149.28, 149.25, 142.58, 137.90, 137.66, 137.07, 132.71, 130.83, 130.20, 128.51, 127.41, 124.12, 121.52, 119.12. MS (MALDI-TOF, dithranol, *m*/*z*): 414.17, $C_{28}H_{20}N_3O$ ($[M + H]^+$) requires 414.16. Anal. Calcd for $C_{28}H_{19}N_3O\cdot H_2O$: C, 77.94; H, 4.91; N, 9.74. Found: C, 77.68; H, 4.81; N, 9.56. UV−vis (CH_2Cl_2): λ_{max}/nm (ε/L mol^{-1} cm^{-1}) 284 (57700).

*Bis(4‴,4⁗-[2,2′:6′,2″]terpyridin-4′-yl)benzophenone (**6c**).* According to the general procedure for Kröhnke-type terpyridine synthesis, 2-acetylpyridine (0.671 g, 5.54 mmol), bis(4,4′-formyl)-benzophenone (**5c**; 0.3 g, 1.26 mmol), and sodium hydroxide (0.222 g, 5.54 mmol) were reacted to yield a beige solid (180 mg, 0.279 mmol, 22%). Mp: >250 °C dec. ^{1}H NMR (300 MHz, $CDCl_3$, ppm): δ 8.80 (s, 4H, H^{D3}), 8.74 (d, ^3J = 4.1 Hz, 4H, H^{C6}), 8.69 (d, ^3J = 7.9 Hz, 4H, H^{C3}), 8.05 (d, ^3J = 8.3 Hz, 4H, H^{E3}), 7.99 (d, ^3J = 8.3 Hz, 4H, H^{E2}), 7.89 (td, ^3J = 7.8 Hz, ^4J = 1.3 Hz, 4H, H^{C4}), 7.37 (dd, ^3J = 6.6 Hz, ^3J = 5.2 Hz, 4H, H^{C5}). ^{13}C NMR (75 MHz, $CDCl_3$, ppm): δ 195.84, 156.33, 156.14, 149.34, 149.26, 142.79, 137.84, 137.07, 130.87, 127.54, 124.13, 121.54, 119.17. MS (MALDI-TOF, dithranol, *m*/*z*): 645.21, $C_{43}H_{29}N_6O$ ($[M + H]^+$) requires 645.24. Anal. Calcd for $C_{43}H_{28}N_6O \times 2\ H_2O$: C, 75.87; H, 4.74; N, 12.35. Found: C, 75.63; H, 4.87. N, 12.33. UV−vis (CH_2Cl_2): λ_{max}/nm (ε/L mol^{-1} cm^{-1}) 285 (68300).

*4-Bromo-2,5-bis(octyloxy)benzophenone (**5b**).* A solution of 2-bromo-1,4-bis(octyloxy)benzene (**4b**; 400 mg, 0.968 mmol) and benzoyl chloride (204 mg, 1.451 mmol) in dichloromethane (5 mL) was stirred at 0 °C under nitrogen, while a mixture of aluminum(III) trichloride (194 mg, 1.451 mmol) was slowly added. The solution was stirred overnight at room temperature before being poured onto iced 2 M HCl solution (50 mL). The dichloromethane layer was separated, and the aqueous phase was extracted with dichloromethane (3 × 30 mL). The combined organic layers were dried over Na_2SO_4, and the organic solvents were removed under reduced pressure. The solid residue was dissolved in dichloromethane (100 mL) and washed successively with 2 M sodium hydroxide solution (3 × 30 mL) and brine (50 mL) before the solution was dried and evaporated. The residue was purified by column chromatography (silica, *n*-hexane/dichloromethane 2/1) to yield a yellow viscous liquid (277 mg, 0.683 mmol, 71%). ^{1}H NMR indicated the formation of 4-bromo-5-hydroxy-2-octyloxybenzophenone by the loss of one octyloxy group during the reaction. The group was reintroduced according to the literature procedure. Therefore, KOH powder (190 mg, 3.38 mmol) was stirred in dried DMSO (6 mL) and the solution was deaerated. 4-Bromo-5-hydroxy-2-octyloxybenzophenone (274 mg, 0.676 mmol) in DMSO (1.5 mL) and 1-bromooctane (259 μL, 1.487 mmol) in DMSO (1.5 mL) were added. The mixture was stirred for 22 h at room temperature. The resulting solid was filtered off and dissolved in toluene (50 mL). The toluene solution was extracted with water (3 × 20 mL) and dried with Na_2SO_4, and the organic solvent was removed under reduced pressure. The residue was purified by column chromatography (silica, *n*-hexane/dichloromethane 1/1) to yield a low-melting white solid (312 mg, 0.603 mmol, 89%, 62% overall yield). Mp: 40 °C. ^{1}H NMR (300 MHz, CD_2Cl_2, ppm): δ 7.80−7.72 (m, 2H, H^{G2}), 7.60−7.52 (m, 1H, H^{G4}), 7.48−7.40 (m, 2H, H^{G3}), 7.22 (s, 1H, H^{F3}), 7.02 (s, 1H, H^{F6}), 4.00 (t, ^3J = 6.5 Hz, 2H, α-OCH_2), 3.80 (t, ^3J = 6.3 Hz, 2H, α-OCH_2), 1.89−1.75 (m, 2H, β-CH_2), 1.58−1.44 (m, 2H, β-CH_2), 1.44−1.05 (m, 20H, γ-η-CH_2), 1.04−0.84 (m, 6H, CH_3). ^{13}C NMR (75 MHz, CD_2Cl_2, ppm): δ 196.02, 151.70, 150.45, 138.83, 133.37, 129.92, 129.29, 128.79, 118.60, 115.96, 114.91, 70.71, 69.94, 32.45, 32.38, 29.91, 29.87, 29.81, 29.76, 29.69, 29.50, 26.59, 26.19, 23.30, 23.27, 14.52, 14.51. HRMS (ESI-TOF, *m*/*z*): 517.2300, $C_{29}H_{42}BrO_3$ ($[M + H]^+$) requires 517.2312.

General Procedure for Sonogashira Cross-Coupling Reactions. Copper(I) iodide (0.1−0.15 equiv) and $[Pd(PPh_3)_4]$ (0.1−0.15 equiv) were added to a deaerated solution of an aromatic bromine (1 equiv) in a mixture of THF (10 mL) and triethylamine (5 mL). With vigorous stirring, 4′-(4-ethynylphenyl)-2,2′:6′,2″-terpyridine (1.2 equiv) in THF (2 mL) was added. Subsequently, the reaction mixture was heated to 60 °C for 48−72 h. After the mixture was cooled to room temperature, the precipitated ammonia salt was filtered off and washed intensely with THF, and the solvent was removed under reduced pressure. Dichloromethane was added, and the solution was washed with saturated aqueous ammonium chloride/EDTA (1/1) solution and dried with Na_2SO_4. Further purification was achieved by column chromatography (neutral alumina, dichloromethane/*n*-hexane).

*2,5-Bis(octyloxy)-4-(4-[2,2′:6′,2″]terpyridin-4′-ylphenylethynyl)-benzophenone (**6b**).* According to the general procedure for Sonogashira cross-coupling reactions, copper(I) iodide (16.6 mg, 0.087 mmol), $[Pd(PPh_3)_4]$ (100 mg, 0.087 mmol), 4-bromo-2,5-bis(octyloxy)benzophenone (**5b**; 300 mg, 0.580 mmol), and 4′-(4-ethynylphenyl)-2,2′:6′,2″-terpyridine (232 mg, 0.696 mmol) were reacted for 72 h. Further purification was achieved by column chromatography (neutral alumina, dichloromethane/*n*-hexane 2/1) to yield an off-white solid (252 mg, 0.327 mmol, 57%). Mp: 110−112 °C. ^{1}H NMR (300 MHz, $CDCl_3$, ppm): δ 8.76 (s, 2H, H^{D3}), 8.74 (d, ^3J = 4.7 Hz, 2H, H^{C6}), 8.68 (d, ^3J = 7.9 Hz, 2H, H^{C3}), 7.93 (d, ^3J = 8.5 Hz, 2H, H^{E2}), 7.89 (td, ^3J = 7.7 Hz, ^4J = 1.7 Hz, 2H, H^{C4}), 7.82−7.77 (m, 2H, H^{G2}), 7.70 (d, ^3J = 8.4 Hz, 2H, H^{E3}), 7.55 (t, ^3J = 7.3 Hz, 1H, H^{G4}), 7.43 (t, ^3J = 7.5 Hz, 2H, H^{G3}), 7.36 (ddd, ^3J = 7.4 Hz, ^3J = 4.8 Hz, ^4J = 1.0 Hz, 2H, H^{C5}), 7.11 (s, 1H, H^{F3}), 7.01 (s, 1H, H^{F6}), 4.06 (t, ^3J = 6.4 Hz, 2H, OCH_2−), 3.84 (t, ^3J = 6.3 Hz, 2H, α-OCH_2), 1.93−1.80 (m, 2H, β-CH_2), 1.63−1.49 (m, 2H, β-CH_2), 1.46−0.93 (m, 20H, γ-η-CH_2), 0.93−0.81 (m, 6H, CH_3). ^{13}C NMR (75 MHz, $CDCl_3$, ppm): δ 196.32, 156.26, 156.19, 154.17, 150.81, 149.51, 149.27, 138.46, 138.41, 137.06, 132.90, 132.33, 130.00, 129.63, 128.29, 127.41, 124.23, 124.05, 121.52, 118.80, 117.27, 116.26, 113.99, 94.91, 87.21, 69.86, 69.27, 31.96, 31.88, 29.51, 29.48, 29.46, 29.29, 29.20, 29.07, 26.22, 25.75, 22.82, 22.77, 14.23, 14.23. HRMS (ESI-TOF, *m*/*z*): 792.4076, $C_{52}H_{55}N_3O_3Na$ ($[M + Na]^+$) requires 792.4136. Anal. Calcd for $C_{52}H_{55}N_3O_3$: C, 81.11; H, 7.20; N, 5.46. Found: C, 81.01; H, 7.30; N, 5.47. UV−vis (CH_2Cl_2): λ_{max}/nm (ε/L mol^{-1} cm^{-1}) 360 (31500), 303 (58000).

*4′-(4-((2,5-Bis(octyloxy)phenyl)ethynyl)phenyl)-2,2′:6′,2″-terpyridine (**11b**).* According to the general procedure for Sonogashira cross-coupling reactions, copper(I) iodide (9.5 mg, 0.050 mmol), $[Pd(PPh_3)_4]$ (0.058 g, 0.050 mmol), 2-bromo-1,4-bis(octyloxy)benzene (**4b**; 207 mg, 0.5 mmol), and 4′-(4-ethynylphenyl)-2,2′:6′,2″-terpyridine (200 mg, 0.600 mmol) were reacted for 48 h. Further purification was achieved by column chromatography (neutral alumina, dichloromethane/*n*-hexane 1/2, then 1/1) to yield a white

DOI: 10.1021/ic502431x
Inorg. Chem. 2015, 54, 3159−3171

solid (280 mg, 0.420 mmol, 84%). Mp: 65−67 °C. ^{1}H NMR (300 MHz, $CDCl_3$, ppm): δ 8.76 (s, 2H, H^{D3}), 8.73 (d, ^3J = 4.4 Hz, 2H, H^{C6}), 8.67 (d, ^3J = 8.0 Hz, 2H, H^{C3}), 7.95−7.83 (m, 4H, H^{E2}, H^{C4}), 7.67 (d, ^3J = 8.3 Hz, 2H, H^{E3}), 7.35 (ddd, ^3J = 7.5 Hz, ^3J = 4.8 Hz, ^4J = 1.2 Hz, 2H, H^{C5}), 7.06 (d, ^4J = 1.8 Hz, 1H, H^{F6}), 6.92−6.77 (m, 2H, H^{F4}, H^{F3}), 4.03 (t, ^3J = 6.4 Hz, 2H, α-OCH_2), 3.93 (t, ^3J = 6.5 Hz, 2H, α-OCH_2), 1.93−1.70 (m, 4H, β-CH_2), 1.63−1.20 (m, 20H, γ-η-CH_2), 0.98−0.78 (m, 6H, CH_3). ^{13}C NMR (75 MHz, $CDCl_3$, ppm): δ 156.3, 156.1, 154.4, 153.0, 149.6, 149.3, 138.0, 137.0, 132.2, 127.3, 124.7, 124.0, 121.5, 118.8, 118.5, 117.0, 114.3, 113.6, 93.1, 87.8, 70.0, 68.9, 32.99, 31.97, 29.6, 29.6, 29.5, 29.5, 29.4, 26.3, 26.2, 22.83, 22.81, 14.3. MS (MALDI-TOF, dithranol, m/z): 666.42, $C_{45}H_{52}N_3O_2$ ([M + H]$^+$) requires 666.41. Anal. Calcd for $C_{45}H_{51}N_3O_2$: C, 81.17; H, 7.72; N, 6.31. Found: C, 81.15; H, 8.07; N, 6.47. UV−vis (CH_2Cl_2): λ_{max}/nm (ε/L mol^{-1} cm^{-1}) 338 (27400), 292 (44300) nm.

General Procedure for Hydrazone Condensation Synthesis. A two-neck flask was loaded with benzophenone derivate **6** (1 equiv), *p*-toluenesulfonyl hydrazide (2 equiv), tosylic acid monohydrate (0.05 equiv), and THF or toluene and the mixture heated to reflux for 48 h under nitrogen. After the mixture was cooled to room temperature, the solvent was evaporated and the residue further purified by column chromatography (neutral alumina, chloroform/ethyl acetate 95/5). When applicable, deviations from this general protocol are given below.

*[2,2′:6′,2″]Terpyridin-4′-ylbenzophenone p-Tosyl Hydrazone (**7a**).* According to the general procedure for hydrazone condensation synthesis, 4‴-[2,2′:6′,2″]terpyridin-4′-yl-benzophenone (**6a**; 131 mg, 0.317 mmol), *p*-toluenesulfonyl hydrazide (118 mg, 0.634 mmol), and tosylic acid monohydrate (3 mg, 0.016 mmol) in toluene (10 mL) were reacted to yield a white solid (68 mg, 0.117 mmol, 37%). ^{1}H NMR suggests a mixture of *cis*- and *trans*-hydrazone isomers, which was used directly for the synthesis of **8a**. Mp: >240 °C dec. ^{1}H NMR (300 MHz, $CDCl_3$, ppm): δ 8.79−8.59 (m, 6H, H^{D3}, H^{C6}, H^{C3}), 7.98 (d, ^3J = 8.3 Hz, 1H, H^{E2}), 7.90 (d, ^3J = 8.2 Hz, 2H, Ar^{tosyl}-*H*), 7.92−7.75 (m, 4H, H^{C4}, H^{G2}), 7.59−7.46 (m, 4H, H^{E2}, H^{G3}, H^{G4}), 7.39−7.30 (m, 5H, N*H*, H^{C5}, Ar^{tosyl}-*H*), 7.29−7.24 (m, 1H, H^{E3}), 7.20−7.13 (m, 1H, H^{E3}), 2.43 (two singlets, 3H, Ar^{tosyl}-CH_3). ^{13}C NMR (75 MHz, $CDCl_3$, ppm): 156.27, 156.13, 156.07, 156.03, 153.92, 153.77, 149.41, 149.27, 149.20, 149.06, 144.42, 144.30, 140.54, 139.85, 137.14, 137.05, 136.48, 135.69, 135.59, 131.79, 131.06, 130.36, 130.09, 129.94, 129.85, 129.83, 129.17, 128.73, 128.46, 128.42, 128.26, 128.11, 128.09, 127.76, 127.24, 124.12, 124.02, 121.50, 119.01, 118.83, 21.77, 21.76. HRMS (ESI-TOF, m/z): 582.1903, $C_{35}H_{28}N_5O_2S$ ([M + H]$^+$) requires 582.1958. Anal. Calcd for $C_{35}H_{27}N_5O_2S{\cdot}H_2O$: C, 70.10; H, 4.87; N, 11.68; S, 5.35. Found: C, 69.93; H, 4.71; N, 11.32; S, 5.16.

*2,5-Bis(octyloxy)-4-(4-[2,2′:6′,2″]terpyridin-4′-yl-phenylethynyl)-benzophenone p-Tosyl Hydrazone (**7b**).* According to the general procedure for hydrazone condensation synthesis, 2,5-bis(octyloxy)-4-(4-[2,2′:6′,2″]terpyridin-4′-ylphenylethynyl)benzophenone (**6b**; 100 mg, 0.130 mmol), *p*-toluenesulfonyl hydrazide (48 mg, 0.260 mmol), and tosylic acid monohydrate (1.2 mg, 6.5 μmol) were reacted in THF (10 mL) for 11 days. The reaction was monitored by MALDI-TOF MS. After 6 days, additional *p*-toluenesulfonyl hydrazide (1 equiv) and tosylic acid monohydrate (0.1 equiv) were added. After purification by column chromatography (neutral alumina, chloroform) and recrystallization (*n*-hexane), a white solid (74 mg, 0.079 mmol, 61%) was obtained. ^{1}H NMR suggests a mixture of *cis*- and *trans*-hydrazone isomers, which was used directly for the synthesis of **8b**. Mp: 83 °C. ^{1}H NMR (300 MHz, $CDCl_3$, ppm): δ 8.81−8.65 (m, 6H, H^{D3}, H^{C6}, H^{C3}), 8.01−7.84 (m, 6H, Ar^{tosyl}-*H*, H^{E2}, H^{C4}), 7.77 (s, 1H, N*H*), 7.70 (d, ^3J = 8.4 Hz, 2H, H^{E3}), 7.57−7.47 (m, 2H, H^{G2}), 7.42−7.27 (m, 7H, H^{C5}, H^{G3}, H^{G4}, Ar^{tosyl}-*H*), 7.16 (s, 1H, H^{F3}), 6.51 (s, 1H, H^{F6}), 3.91 (t, ^3J = 6.4 Hz, 2H, α-OCH_2), 3.79 (t, ^3J = 6.3 Hz, 2H, α-OCH_2), 2.41 (s, 3H, Ar^{tosyl}−CH_3), 1.75−1.46 (m, 4H, β-CH_2), 1.46−0.93 (m, 20H, γ−η−CH_2), 0.95−0.78 (m, 6H, CH_3); ^{13}C NMR (75 MHz, $CDCl_3$, ppm): δ 156.26, 156.22, 154.69, 151.75, 149.48, 149.42, 149.28, 143.92, 138.56, 137.04, 136.66, 136.04, 132.35, 129.77, 129.68, 129.62, 129.18, 128.34, 128.32, 128.13, 127.53, 127.43, 127.37, 124.05, 121.64, 121.52, 118.79, 118.20, 115.91, 113.78, 94.86, 86.70, 69.85, 69.82, 32.00, 31.94, 31.84, 29.49, 29.44, 29.40, 29.26, 29.20, 28.93, 26.18, 25.65, 22.81, 22.76, 21.72, 14.23, 14.22. MS (MALDI-TOF, dithranol, m/z): 938.43, $C_{59}H_{64}N_5O_4S$ ([M + H]$^+$) requires 938.47.

*Bis(4‴,4′′′′-[2,2′:6′,2″]terpyridin-4′-yl)benzophenone p-Tosyl Hydrazone (**7c**).* According to the general procedure for hydrazone condensation synthesis, bis(4‴,4′′′′-[2,2′:6′,2″]terpyridin-4′-yl)-benzophenone (**6c**; 120 mg, 0.186 mmol), *p*-toluenesulfonyl hydrazide (69 mg, 0.372 mmol), and tosylic acid monohydrate (2 mg, 0.011 mmol) were reacted in toluene (10 mL) to yield a white solid (60 mg, 0.074 mmol, 40%). Mp >240 °C dec. ^{1}H NMR (300 MHz, $CDCl_3$, ppm): δ 8.79−8.61 (m, 12H, H^{D3}, H^{C6}, H^{C3}), 8.26−8.14 (m, 1H, N*H*), 8.02−7.94 (m, 4H, H^{E2}), 7.93−7.81 (m, 4H, H^{C4}), 7.77 (d, ^3J = 8.5 Hz, 2H, Ar^{tosyl}-*H*), 7.59 (d, ^3J = 8.4 Hz, 2H, Ar^{tosyl}-*H*), 7.44−7.28 (m, 8H, H^{E3}, H^{C5}), 2.45 (s, 3H, Ar^{tosyl}-CH_3). ^{13}C NMR (75 MHz, $CDCl_3$, ppm): δ 156.29, 156.13, 156.07, 153.32, 149.39, 149.30, 149.23, 149.08, 144.53, 140.68, 139.92, 137.07, 135.68, 131.60, 129.95, 129.28, 128.76, 128.35, 128.21, 127.30, 124.12, 124.03, 121.54, 121.50, 119.09, 118.87, 29.83; MS (MALDI-TOF, dithranol, m/z): 813.29, $C_{50}H_{37}N_8O_2S$ ([M + H]$^+$) requires 813.28.

General Procedure for Methanofullerene Synthesis. To a solution of the *p*-tosyl hydrazone derivate **7** (1 equiv) in anhydrous pyridine (3 mL) was added sodium methoxide (1.1 equiv) under a nitrogen atmosphere. After the mixture was stirred at room temperature for 15 min, a nitrogen-purged solution of C_{60} (3−4 equiv) in *o*-dichlorobenzene (15 mL) was added at once and the mixture was heated to 180 °C for 24 h. After it was cooled to room temperature, the reaction mixture was purified by column chromatography (neutral alumina, toluene/*n*-hexane 1/1) and precipitation in methanol.

*1-Phenyl-1-(4-[2,2′:6′,2″]terpyridin-4′-ylphenyl)methanofullerene (**8a**).* According to the general procedure for methanofullerene synthesis, [2,2′:6′,2″]terpyridin-4′-yl-benzophenone *p*-tosyl hydrazone (**7a**; 60 mg, 0.103 mmol), sodium methoxide (6 mg, 0.111 mmol), and C_{60} (276 mg, 0.383 mmol) were reacted to yield a brown solid (32 mg, 0.029 mmol, 28%). Mp: >360 °C. ^{1}H NMR (300 MHz, $CDCl_3$, ppm): δ 8.79 (s, 2H, H^{D3}), 8.73 (d, ^3J = 4.8 Hz, 2H, H^{C6}), 8.69 (d, ^3J = 7.9 Hz, 2H, H^{C3}), 8.27 (d, ^3J = 8.3 Hz, 2H, H^{E2}), 8.22−8.15 (m, 2H, H^{G2}), 8.02 (d, ^3J = 8.3 Hz, 2H, H^{E3}), 7.90 (td, ^3J = 7.8 Hz, ^4J = 1.8 Hz, 2H, H^{C4}), 7.53 (t, ^3J = 7.5 Hz, 2H, H^{G3}), 7.46−7.33 (m, 3H, H^{G4}, H^{C5}). MS (MALDI-TOF, negative mode, terthiophene, m/z): 1117.14, $C_{88}H_{19}N_3$ ([M + e]$^-$) requires 1117.16. Anal. Calcd for $C_{88}H_{19}N_3{\cdot}2.5H_2O{\cdot}3$(hexane): C, 89.55; H, 4.68; N, 2.96. Found: C, 89.57; H, 4.51; N, 3.01.

*1-Phenyl-1-(2,5-Bis(octyloxy)-4-(4-[2,2′:6′,2″]terpyridin-4′-ylphenylethynyl))methanofullerene (**8b**).* According to the general procedure for methanofullerene synthesis, 2,5-bis(octyloxy)-4-(4-[2,2′:6′,2″]terpyridin-4′-ylphenylethynyl)benzophenone *p*-tosyl hydrazone (**7b**; 57 mg, 0.061 mmol), sodium methoxide (4 mg, 0.074 mmol), and C_{60} (175 mg, 0.243 mmol) were reacted to yield a dark brown solid (24 mg, 0.016 mmol, 27%). Mp: 148 °C. ^{1}H NMR (300 MHz, $CDCl_3$, ppm): δ 8.76 (s, 2H, H^{D3}), 8.74 (d, ^3J = 4.8 Hz, 2H, H^{C6}), 8.68 (d, ^3J = 7.9 Hz, 2H, H^{C3}), 8.24 (d, ^3J = 7.1 Hz, 2H, H^{G2}), 7.96−7.82 (m, 4H, H^{E2}, H^{C4}), 7.68 (d, ^3J = 8.2 Hz, 2H, H^{E3}), 7.64 (s, 1H, H^{F6}), 7.50 (t, ^3J = 7.3 Hz, 2H, H^{G3}), 7.46−7.38 (m, 1H, H^{G4}), 7.36 (dd, ^3J = 6.8 Hz, ^3J = 5.4 Hz, 2H, H^{C5}), 7.18 (s, 1H, H^{F3}), 4.27−3.98 (m, 4H, α-OCH_2), 2.13−1.99 (m, 2H, β-CH_2), 1.93−1.78 (m, 2H, β-CH_2), 1.75−1.10 (m, 20H, γ-η-CH_2), 0.97−0.79 (m, 6H, CH_3). MS (MALDI-TOF, negative mode, terthiophene, m/z): 1473.38, $C_{112}H_{55}N_3O_2$ ([M + e]$^-$) requires 1473.43. Anal. Calcd for $C_{112}H_{55}N_3O_2{\cdot}8H_2O$: C, 83.10; H, 4.42%; N, 2.60. Found: C, 83.34; H, 4.47; N, 2.49.

*1,1-Bis(4-[2,2′:6′,2″]terpyridin-4′-ylphenyl)methanofullerene (**8c**).* According to the general procedure for methanofullerene synthesis, bis(4‴,4′′′′-[2,2′:6′,2″]terpyridin-4′-yl)benzophenone *p*-tosyl hydrazone (**7c**; 60 mg, 0.074 mmol), sodium methoxide (4 mg, 0.074 mmol), and C_{60} (227 mg, 0.315 mmol) were reacted to yield a brown solid (30 mg, 0.022 mmol, 30%). Mp: >360 °C. ^{1}H NMR (300 MHz, $CDCl_3$, ppm): δ 8.79 (s, 4H, H^{D3}), 8.73 (d, ^3J = 4.0 Hz, 4H, H^{C6}), 8.68 (d, ^3J = 8.0 Hz, 4H, H^{C3}), 8.31 (d, ^3J = 8.2 Hz, 4H, H^{E2}), 8.04 (d, ^3J = 8.2 Hz, 4H, H^{E3}), 7.88 (td, ^3J = 7.7 Hz, ^4J = 1.7 Hz, 4H, H^{C4}), 7.35 (ddd, ^3J = 7.4 Hz, ^3J = 4.8 Hz, ^4J = 0.9 Hz, 4H, H^{C5}). MS (MALDI-

DOI: 10.1021/ic502431x
Inorg. Chem. 2015, 54, 3159−3171

TOF, negative mode, terthiophene, m/z): 1348.23, $C_{103}H_{28}N_6$ ([M + e]$^-$) requires 1348.24. Anal. Calcd for $C_{103}H_{28}N_6{\cdot}4H_2O{\cdot}5$(hexane): C, 86.24; H, 5.77; N, 4.54. Found: C, 86.11; H, 5.48; N, 4.44.

*N-Methyl-2-(4-[2,2′:6′,2″]terpyridin-4′-ylphenyl)-pyrrolidinofullerene (**10a**).* A mixture of (4-formylphenyl)-2,2′:6′,2″-terpyridine (**9a**; 33 mg, 0.098 mmol), *N*-methylglycine (87 mg, 0.978 mmol), and C_{60} (282 mg, 0.391 mmol) in deaerated, anhydrous toluene (200 mL) was stirred at 120 °C for 24 h under a nitrogen atmosphere. After the mixture was cooled to room temperature, the solvent was evaporated. The crude product was purified by column chromatography (neutral alumina, toluene then chloroform), and slow vapor diffusion of diethyl ether into a concentrated solution yielded a brown solid (26.5 mg, 0.024 mmol, 25%). Mp: >360 °C. ^{1}H NMR (300 MHz, $CDCl_3$, ppm): δ 8.74 (s, 2H, H^{D3}), 8.72 (d, ^3J = 4.8 Hz, 2H, H^{C6}), 8.67 (d, ^3J = 7.9 Hz, 2H, H^{C3}), 8.00−7.93 (m, 4H, H^{E2}, H^{E3}), 7.87 (td, ^3J = 7.8 Hz, ^4J = 1.7 Hz, 2H, H^{C4}), 7.35 (ddd, ^3J = 7.5 Hz, ^3J = 4.8 Hz, ^4J = 1.1 Hz, 2H, H^{C5}), 5.02 (d, ^2J = 9.2 Hz, 1H, H^{H5}), 5.02 (s, 1H, H^{H2}), 4.30 (d, ^2J = 9.5 Hz, 1H, H^{H5}), 2.85 (s, 3H, NCH_3). MS (MALDI-TOF, negative mode, terthiophene, m/z): 1083.26, $C_{84}H_{19}N_4$ ([M − H]$^-$) requires 1083.16. Anal. Calcd for $C_{84}H_{20}N_4{\cdot}6H_2O$: C, 84.56; H, 2.70; N, 4.70. Found: C, 84.26; H, 2.44; N, 5.40.

*N-Methyl-2-(2,5-Bis(octyloxy)-4-(4-[2,2′:6′,2″]terpyridin-4′-ylphenylethynyl))pyrrolidinofullerene (**10b**).* A mixture of 2,5-bis-(octyloxy)-4-(4-[2,2′:6′,2″]-terpyridin-4′-ylphenylethynyl)-benzaldehyde (**9b**; 69 mg, 0.1 mmol), *N*-methylglycine (89 mg, 1.0 mmol), and C_{60} (144 mg, 0.2 mmol) in deaerated, anhydrous toluene (200 mL) was stirred at 120 °C for 24 h under a nitrogen atmosphere. After the mixture was cooled to room temperature, the solvent was evaporated. The crude product was purified by column chromatography (neutral alumina, *n*-hexane/toluene 3/1 then toluene) to yield a dark brown-black solid (101 mg, 0.07 mmol, 70%). Mp: 155 °C. ^{1}H NMR (400 MHz, CD_2Cl_2, ppm): δ 8.77 (s, 2H, H^{D3}), 8.71 (d, ^3J = 4.7 Hz, 2H, H^{C6}), 8.68 (d, ^3J = 7.9 Hz, 2H, H^{C3}), 7.93−7.86 (m, 4H, H^{E2}, H^{C4}), 7.67 (d, ^3J = 8.5 Hz, 2H, H^{E3}), 7.65 (s, 1H, H^{F5}), 7.37 (ddd, ^3J = 7.4 Hz, ^3J = 4.8 Hz, ^4J = 1.1 Hz, 2H, H^{C5}), 7.09 (s, 1H, H^{F2}), 5.58 (s, 1H, H^{H2}), 4.97 (d, ^2J = 9.4 Hz, 1H, H^{H5}), 4.33 (d, ^2J = 9.5 Hz, 1H, H^{H5}), 4.20 (dt, ^2J = 9.5 Hz, ^3J = 6.6 Hz, 1H, α-OCH_2), 4.10 (dt, ^2J = 9.6 Hz, ^3J = 6.4 Hz, 1H, α-OCH_2), 4.03 (dt, ^2J = 13.1 Hz, ^3J = 6.5 Hz, 1H, α-OCH_2), 3.74 (dt, ^2J = 8.6 Hz, ^3J = 6.5 Hz, 1H, α-OCH_2), 2.83 (s, 3H, NCH_3), 1.87−1.76 (m, 2H, β-CH_2), 1.73−1.49 (m, 6H, β-CH_2, γ-CH_2), 1.48−1.17 (m, 16H, δ-η-CH_2), 0.96−0.73 (m, 6H, CH_3). ^{13}C NMR (100 MHz, CD_2Cl_2, ppm): δ 157.34, 156.51, 156.39, 155.57, 154.70, 154.68, 154.36, 152.03, 149.59, 149.58, 147.66, 147.22, 147.15, 146.62, 146.60, 146.56, 146.47, 146.43, 146.41, 146.32, 146.31, 146.14, 145.99, 145.90, 145.66, 145.64, 145.60, 145.58, 145.54, 145.48, 144.97, 144.92, 144.85, 144.72, 143.40, 143.36, 143.03, 142.99, 142.91, 142.74, 142.70, 142.62, 142.57, 142.50, 142.49, 142.47, 142.34, 142.19, 142.10, 142.08, 140.50, 140.45, 139.97, 139.91, 137.24, 136.83, 136.76, 136.54, 135.09, 132.45, 128.24, 127.65, 124.72, 124.34, 121.50, 118.88, 116.49, 115.24, 113.12, 93.52, 88.23, 77.05, 76.00, 70.33, 70.17, 69.77, 69.21, 40.24, 32.35, 32.32, 30.11, 29.93, 29.90, 29.82, 29.74, 29.73, 29.67, 26.55, 26.48, 23.19, 23.14, 21.55, 14.40, 14.35. MS (MALDI-TOF, negative mode, terthiophene, m/z): 1440.42, $C_{108}H_{56}N_4O_2$ ([M + e]$^-$) requires 1440.44. Anal. Calcd for $C_{108}H_{56}N_4O_2{\cdot}0.5$(hexane): C, 89.79; H, 4.28; N, 3.77. Found: C, 89.78; H, 4.43; N, 3.83.

General Procedure for the Synthesis of Heteroleptic Ruthenium Bis(terpyridine) Complexes. A microwave vial was charged with [Ru(tpy)(MeCN)$_3$](PF$_6$)$_2$ (1 equiv per terpyridine group), terpyridine derivative (1 equiv), and DMF (3 mL). The vial was capped, purged with nitrogen for 20 min, and heated through microwave irradiation at 140 °C for 30 min. Subsequently, the solution was cooled to room temperature and the product was precipitated by addition of an aqueous ammonium hexafluorophosphate solution. The solid was collected by filtration, washed thoroughly with water and diethyl ether, and dissolved in acetonitrile. The solution was concentrated and treated with diethyl ether vapor to slowly precipitate the complex. When applicable, deviations from this general protocol are given below.

*[Ru(tpy)(**8a**)](PF$_6$)$_2$ (**1a**).* According to the general procedure for heteroleptic ruthenium bis(terpyridine) complexes, [Ru(tpy)(MeCN)$_3$](PF$_6$)$_2$ (6.4 mg, 8.5 μmol) and **8a** (9.4 mg, 8.4 μmol) were reacted to yield a dark red solid (6 mg, 3.4 μmol, 41%). ^{1}H NMR (400 MHz, CD_3CN, ppm): δ 9.02 (s, 2H, H^{D3}), 8.75 (d, ^3J = 8.2 Hz, 2H, H^{B3}), 8.69−8.57 (m, 4H, H^{E2}, H^{C3}), 8.48 (d, ^3J = 8.1 Hz, 2H, H^{A3}), 8.41 (t, ^3J = 8.1 Hz, 1H, H^{B4}), 8.35 (d, ^3J = 7.2 Hz, 4H, H^{G2}, H^{E3}), 8.00−7.80 (m, 4H, H^{C4}, H^{A4}), 7.61−7.48 (m, 2H, H^{G3}), 7.49−7.39 (m, 1H, H^{G4}), 7.38−7.30 (m, 4H, H^{A6}, H^{C6}), 7.21−7.01 (m, 4H, H^{C5}, H^{A5}). ^{13}C NMR (100 MHz, CD_3CN, ppm): δ 159.05, 159.00, 156.47, 156.28, 153.58, 153.22, 149.57, 149.52, 148.25, 146.94, 146.80, 146.20, 145.72, 145.70, 145.61, 145.36, 145.27, 144.83, 143.96, 143.89, 143.17, 143.08, 142.46, 141.83, 139.77, 139.10, 139.01, 138.84, 138.69, 137.71, 136.89, 133.19, 132.11, 130.11, 129.73, 129.38, 128.52, 128.47, 125.49, 124.76, 122.70, 80.14, 58.87. HRMS (ESI-TOF, m/z): 726.0829, $C_{103}H_{30}N_6Ru$ ([M − 2PF$_6$]$^{2+}$) requires 726.0785.

*[Ru(tpy)(**8b**)](PF$_6$)$_2$ (**1b**).* According to the general procedure for heteroleptic ruthenium bis(terpyridine) complexes, [Ru(tpy)(MeCN)$_3$](PF$_6$)$_2$ (6.4 mg, 8.5 μmol) and **8b** (9 mg, 6.1 μmol) were reacted to yield a dark red solid (4 mg, 1.9 μmol, 31%). ^{1}H NMR (300 MHz, CD_3CN, ppm): δ 8.96 (s, 2H, H^{D3}), 8.75 (d, ^3J = 8.2 Hz, 2H, H^{B3}), 8.59 (d, ^3J = 7.3 Hz, 2H, 2H, H^{C3}), 8.49 (d, ^3J = 8.3 Hz, 2H, H^{A3}), 8.41 (t, ^3J = 8.1 Hz, 1H, H^{B4}), 8.35 (d, ^3J = 5.8 Hz, 2H, H^{G2}), 8.21 (d, ^3J = 7.5 Hz, 2H, H^{E2}), 7.99−7.78 (m, 7H, H^{E3}, H^{F6}, H^{C4}, H^{A4}), 7.56−7.39 (m, 3H, H^{G3}, H^{G4}), 7.39 (d, ^3J = 5.2 Hz, 2H, H^{A6}), 7.34 (d, ^3J = 5.3 Hz, 2H, H^{C6}), 7.25 (s, 1H, H^{F3}), 7.21−7.07 (m, 4H, H^{C5}, H^{A5}), 4.29−4.10 (m, 3H, α-OCH_2), 4.08−3.92 (m, 1H, α-OCH_2), 1.85−1.59 (m, 4H, β-CH_2), 1.55−1.02 (m, 20H, γ-η-CH_2), 0.91−0.67 (m, 6H, CH_3). HRMS (ESI-TOF, m/z): 904.2109, $C_{127}H_{66}N_6O_2Ru$ ([M − 2PF$_6$]$^{2+}$) requires 904.2143.

*[Ru$_2$(tpy)$_2$(**8c**)](PF$_6$)$_4$ (**1c**).* According to the general procedure for heteroleptic ruthenium bis(terpyridine) complexes, [Ru(tpy)(MeCN)$_3$](PF$_6$)$_2$ (9.7 mg, 13 μmol) and **8c** (8.7 mg, 6.5 μmol) were reacted to yield a dark red solid (8 mg, 3.1 μmol, 48%). ^{1}H NMR (300 MHz, CD_3CN, ppm): δ 9.08 (s, 4H, H^{D3}), 8.80 (d, ^3J = 8.1 Hz, 4H, H^{E2}), 8.75 (d, ^3J = 8.2 Hz, 4H, H^{B3}), 8.67 (d, ^3J = 7.9 Hz, 4H, H^{C3}), 8.54−8.37 (m, 10H, H^{A3}, H^{E3}, H^{B4}), 8.00−7.86 (m, 8H, H^{C4}, H^{A4}), 7.42 (d, ^3J = 5.2 Hz, 4H, H^{A6}), 7.36 (d, ^3J = 5.2 Hz, 4H, H^{C6}), 7.23−7.10 (m, 8H, H^{C5}, H^{A5}). ^{13}C NMR (63 MHz, CD_3CN, ppm): δ 159.07, 156.56, 156.33, 153.58, 153.32, 149.39, 148.32, 146.92, 146.27, 146.24, 145.74, 145.68, 145.46, 144.86, 144.05, 143.98, 143.15, 143.07, 141.96, 141.91, 139.13, 139.06, 138.81, 138.09, 136.89, 133.46, 129.54, 128.54, 128.49, 125.58, 125.47, 124.76, 122.76, 79.99, 58.28. HRMS (ESI-TOF, m/z): 504.5643, $C_{133}H_{50}N_{12}Ru_2$ ([M − 4PF$_6$]$^{4+}$) requires 504.5599.

*[Ru(tpy)(**10a**)](PF$_6$)$_2$ (**2a**).* According to the general procedure for heteroleptic ruthenium bis(terpyridine) complexes, [Ru(tpy)(MeCN)$_3$](PF$_6$)$_2$ (8.9 mg, 12 μmol) and **10a** (13 mg, 12 μmol) were reacted to yield a dark red solid (7 mg, 4.1 μmol, 34%). ^{1}H NMR (300 MHz, CD_3CN, ppm): δ 9.00 (s, 2H, H^{D3}), 8.74 (d, ^3J = 8.2 Hz, 2H, H^{B3}), 8.62 (d, ^3J = 7.8 Hz, 2H, H^{C3}), 8.48 (d, ^3J = 8.1 Hz, 2H, H^{A3}), 8.40 (t, ^3J = 8.5 Hz, 1H, H^{B4}), 8.34−8.19 (m, 4H, H^{E2}, H^{E3}), 7.98−7.86 (m, 4H, H^{C4}, H^{A4}), 7.40 (d, ^3J = 5.5 Hz, 2H, H^{A6}), 7.32 (d, ^3J = 5.1 Hz, 2H, H^{C6}), 7.21−7.08 (m, 4H, H^{C5}, H^{A5}), 5.29 (s, 1H, H^{H2}), 5.14 (d, ^2J = 9.5 Hz, 1H, H^{H5}), 4.44 (d, ^2J = 9.7 Hz, 1H, H^{H5}), 2.91 (s, 3H, NCH_3). HRMS (ESI-TOF, m/z): 709.5853, $C_{99}H_{31}N_7Ru$ ([M − 2PF$_6$]$^{2+}$) requires 709.5839.

*[Ru(tpy)(**10b**)](PF$_6$)$_2$ (**2b**).* According to the general procedure for heteroleptic ruthenium bis(terpyridine) complexes, [Ru(tpy)(MeCN)$_3$](PF$_6$)$_2$ (15.6 mg, 21 μmol) and **10b** (30 mg, 21 μmol) were reacted to yield a dark red solid (23 mg, 11 μmol, 54%). ^{1}H NMR (400 MHz, CD_2Cl_2, ppm): δ 8.83 (s, 2H, H^{D3}), 8.69 (d, ^3J = 8.1 Hz, 2H, H^{B3}), 8.51 (d, ^3J = 7.8 Hz, 2H, H^{C3}), 8.48−8.36 (m, 3H, H^{B4}, H^{A3}), 8.12 (d, ^3J = 8.0 Hz, 2H, H^{E2}), 7.99−7.87 (m, 4H, H^{C4}, H^{A4}), 7.86 (d, ^3J = 7.9 Hz, 2H, H^{E3}), 7.69 (s, 1H, H^{F5}), 7.39 (d, ^3J = 5.4 Hz, 2H, H^{A6}), 7.32 (d, ^3J = 5.7 Hz, 2H, H^{C6}), 7.26−7.17 (m, 4H, H^{C5}, H^{A5}), 7.14 (s, 1H, H^{F2}), 5.61 (s, 1H, H^{H2}), 5.01 (d, ^2J = 9.6 Hz, 1H, H^{H5}), 4.37 (d, ^2J = 9.4 Hz, 1H, H^{H5}), 4.28−4.18 (m, 1H, α-OCH_2), 4.18−4.09 (m, 1H, α-OCH_2), 4.10−4.00 (m, 1H, α-OCH_2), 3.82−3.71 (m, 1H, α-OCH_2), 2.86 (s, 3H, NCH_3), 1.90−1.78 (m, 2H, β-CH_2), 1.73−1.12 (m, 22H, β-CH_2, γ-η-CH_2), 0.94−0.75 (m, 6H, CH_3). ^{13}C NMR (100 MHz, DMSO-d_6, ppm): δ 157.91, 157.74,

DOI: 10.1021/ic502431x
Inorg. Chem. 2015, 54, 3159−3171

157.04, 155.14, 155.00, 154.72, 154.25, 153.91, 153.54, 152.13, 152.07, 151.16, 146.80, 146.69, 146.62, 146.35, 145.74, 145.68, 145.65, 145.63, 145.57, 145.42, 145.25, 145.08, 144.99, 144.79, 144.71, 144.55, 144.49, 144.13, 143.98, 143.92, 143.85, 142.54, 142.16, 142.07, 141.89, 141.84, 141.75, 141.63, 141.49, 141.32, 141.21, 141.11, 139.65, 139.55, 139.43, 138.87, 138.77, 138.14, 138.04, 137.92, 135.85, 135.78, 135.56, 134.34, 133.52, 131.95, 129.63, 129.59, 127.92, 127.79, 127.70, 127.63, 124.88, 124.85, 124.84, 124.58, 124.56, 124.54, 124.02, 120.93, 120.91, 116.41, 114.44, 114.43, 114.40, 112.16, 109.46, 93.04, 88.81, 76.32, 75.05, 69.10, 69.06, 68.47, 40.43, 31.36, 31.30, 29.03, 28.95, 28.80, 28.73, 28.39, 25.49, 25.45, 22.25, 22.13, 14.05, 14.01. HRMS (ESI-TOF, *m*/*z*): 887.7307, $C_{123}H_{67}N_7O_2Ru$ ($[M - 2PF_6]^{2+}$) requires 887.7212.

*[Ru(tpy)(ttpy)](PF$_6$)$_2$ (**3a**)*. According to the general procedure for heteroleptic ruthenium bis(terpyridine) complexes, [Ru(tpy)-(MeCN)$_3$](PF$_6$)$_2$ (58.5 mg, 0.078 mmol) and ttpy (25.3 mg, 0.078 mmol) were reacted in ethanol (5 mL) at 130 °C. Subsequently, the solvent was evaporated and the resulting residue was purified by column chromatography (silica, MeCN/H$_2$O/saturated aqueous KNO$_3$ solution 40/4/1). Concentration of the product fraction in vacuo and precipitation by addition of an aqueous ammonium hexafluorophosphate solution yielded a red solid (56 mg, 0.059 mmol, 76%). ^{1}H NMR (300 MHz, CD$_3$CN, ppm): δ 8.99 (s, 2H, H^{D3}), 8.76 (d, ^3J = 8.1 Hz, 2H, H^{B3}), 8.64 (d, ^3J = 8.1 Hz, 2H, H^{C3}), 8.50 (d, ^3J = 8.1 Hz, 2H, H^{A3}), 8.41 (t, ^3J = 8.1 Hz, 1H, H^{B4}), 8.11 (d, ^3J = 8.1 Hz, 2H, H^{E2}), 8.00−7.87 (m, 4H, H^{C4}, H^{A4}), 7.58 (d, ^3J = 7.9 Hz, 2H, H^{E3}), 7.43 (d, ^3J = 5.5 Hz, 2H, H^{A6}), 7.35 (d, ^3J = 5.4 Hz, 2H, H^{C6}), 7.22−7.11 (m, 4H, H^{C5}, H^{A5}), 2.54 (s, 3H, Ph−CH_3). ^{13}C NMR (75 MHz, CD$_3$CN, ppm): δ 159.20, 159.08, 156.41, 156.38, 153.54, 153.36, 149.42, 142.07, 139.05, 139.01, 136.71, 134.91, 131.30, 128.67, 128.46, 128.42, 125.48, 125.40, 124.70, 122.37, 21.43. Anal. Calcd for $C_{37}H_{28}F_{12}N_6P_2Ru$: C, 46.89; H, 2.98; N, 8.87. Found: C, 46.53; H, 3.02; N, 8.76.

*[Ru(tpy)(**11b**)](PF$_6$)$_2$ (**3b**)*. A mixture of [Ru(tpy)]Cl$_3$ (4.4 mg, 10 μmol) and silver(I) tetrafluoroborate (5.8 mg, 30 μmol) in deaerated acetone (3 mL) was heated to 70 °C for 2 h. After cooling and filtration, DMF (2 mL) was added to the filtrate and the acetone was removed in vacuo. The resulting blue solution of [Ru(tpy)(acetone)$_3$]-(BF$_4$)$_3$ was added to a solution of 4′-(4-((2,5-Bis(octyloxy)phenyl)-ethynyl)phenyl)-2,2′:6′,2″-terpyridine (**11b**; 20 mg, 14 μmol) in DMF (3 mL), and the mixture was heated to 160 °C for 3 h. Subsequently, the reaction mixture was cooled to room temperature and a solid was precipitated by addition of an aqueous ammonium hexafluorophosphate solution. After filtration, the solid was further purified by column chromatography (silica, MeCN/H$_2$O/saturated aqueous KNO$_3$ solution 40/4/1). Concentration of the product fraction in vacuo and precipitation by addition of an aqueous ammonium hexafluorophosphate solution yielded a red solid (10 mg, 7.8 μmol, 78%). ^{1}H NMR (300 MHz, CD$_3$CN, ppm): δ 9.01 (s, 2H, H^{D3}), 8.76 (d, ^3J = 8.2 Hz, 2H, H^{B3}), 8.65 (d, ^3J = 8.0 Hz, 2H, H^{C3}), 8.50 (d, ^3J = 8.0 Hz, 2H, H^{A3}), 8.42 (t, ^3J = 8.1 Hz, 1H, H^{B4}), 8.25 (d, ^3J = 8.5 Hz, 2H, H^{E2}), 8.00−7.84 (m, 6H, H^{C4}, H^{A4}, H^{E3}), 7.42 (d, ^3J = 4.9 Hz, 2H, H^{A6}), 7.36 (d, ^3J = 4.9 Hz, 2H, H^{C6}), 7.22−7.13 (m, 4H, H^{C5}, H^{A5}), 7.09 (d, ^4J = 2.4 Hz, 1H, H^{F6}), 7.02−6.90 (m, 2H, H^{F4}, H^{F3}), 4.08 (t, ^3J = 6.3 Hz, 2H, α-OCH_2), 3.97 (t, ^3J = 6.5 Hz, 2H, α-OCH_2), 1.91−1.68 (m, 4H, β-CH_2), 1.67−1.21 (m, 20H, γ-η-CH_2), 1.01−0.80 (m, 6H, CH_3). ^{13}C NMR (75 MHz, CD$_3$CN, ppm): δ 159.09, 159.05, 156.6, 156.3, 155.2, 153.9, 153.6, 153.4, 148.2, 139.12, 139.07, 137.4, 136.9, 133.4, 129.0, 128.5, 128.5, 126.5, 125.6, 125.4, 124.7, 122.4, 119.5, 118.1, 115.3, 113.7, 93.2, 89.7, 70.4, 69.6, 32.61, 32.59, 30.2, 30.14, 30.11, 30.07, 30.04, 30.02, 26.9, 26.7, 23.5, 23.4, 14.5, 14.4. HRMS (ESI-TOF, *m*/*z*): 500.1984, $C_{60}H_{62}N_6O_2Ru$ ($[M - 2PF_6]^{2+}$) requires 500.1992.

■ ASSOCIATED CONTENT

Ⓢ Supporting Information

Figures S1−S62, giving cyclic voltammograms, absorption and emission spectra, time-resolved data, DFT calculations, NMR data, and MS spectra. This material is available free of charge via the Internet at http://pubs.acs.org.

■ AUTHOR INFORMATION

Corresponding Authors

*E-mail for B.D.: benjamin.dietzek@ipht-jena.de.

*E-mail for U.S.S.: ulrich.schubert@uni-jena.de.

Author Contributions

$^{\perp}$The manuscript was written through contributions of all authors. All authors have given approval to the final version of the manuscript. These authors contributed equally.

Notes

The authors declare no competing financial interest.

■ ACKNOWLEDGMENTS

Financial support by the Deutsche Forschungsgemeinschaft (DFG, Grant Nos. SCHU1229-16/1 and DI1517-3/1) and the Fonds der Chemischen Industrie is kindly acknowledged. Moreover, this project was supported by the COST Action CM1202 Perspect-H2O. The authors also thank Sarah Crotty (MALDI MS), Nicole Fritz (ESI MS), and Sandra Köhn (elemental analysis) for their help with the respective measurements.

■ REFERENCES

(1) Artero, V.; Chavarot-Kerlidou, M.; Fontecave, M. *Angew. Chem., Int. Ed.* **2011**, *50*, 7238.

(2) Andreiadis, E. S.; Chavarot-Kerlidou, M.; Fontecave, M.; Artero, V. *Photochem. Photobiol.* **2011**, *87*, 946.

(3) Artero, V.; Fontecave, M. *Coord. Chem. Rev.* **2005**, *249*, 1518.

(4) Natali, M.; Campagna, S.; Scandola, F. *Chem. Soc. Rev.* **2014**, *43*, 4005.

(5) Sartorel, A.; Bonchio, M.; Campagna, S.; Scandola, F. *Chem. Soc. Rev.* **2013**, *42*, 2262.

(6) Carraro, M.; Sartorel, A.; Toma, F. M.; Puntoriero, F.; Scandola, F.; Campagna, S.; Prato, M.; Bonchio, M. *Top. Curr. Chem.* **2011**, *303*, 121.

(7) Barber, J.; Tran, P. D. *J. R. Soc. Interface* 2013, *10*.

(8) Gust, D.; Moore, T. A.; Moore, A. L. *Acc. Chem. Res.* **2001**, *34*, 40.

(9) Berardi, S.; Drouet, S.; Francàs, L.; Gimbert-Suriñach, C.; Guttentag, M.; Richmond, C.; Stoll, T.; Llobet, A. *Chem. Soc. Rev.* **2014**, *43*, 7501.

(10) Sun, L.; Gao, Y.; Yu, Z.; Ding, X.; Duan, L. *Faraday Discuss.* **2014**, DOI: 10.1039/c4fd00127c.

(11) Fukuzumi, S.; Ohkubo, K.; Suenobu, T. *Acc. Chem. Res.* **2014**, *47*, 1455.

(12) Wenger, O. S. *Chem. Soc. Rev.* **2011**, *40*, 3538.

(13) Schubert, C.; Wielopolski, M.; Mewes, L. H.; de Miguel Rojas, G.; van der Pol, C.; Moss, K. C.; Bryce, M. R.; Moser, J. E.; Clark, T.; Guldi, D. M. *Chem. Eur. J.* **2013**, *19*, 7575.

(14) Guldi, D. M.; Maggini, M.; Scorrano, G.; Prato, M. *J. Am. Chem. Soc.* **1997**, *119*, 974.

(15) Guldi, D. M. *Chem. Soc. Rev.* **2002**, *31*, 22.

(16) Wielopolski, M.; Atienza, C.; Clark, T.; Guldi, D. M.; Martín, N. *Chem. Eur. J.* **2008**, *14*, 6379.

(17) Wielopolski, M.; Santos, J.; Illescas, B. M.; Ortiz, A.; Insuasty, B.; Bauer, T.; Clark, T.; Guldi, D. M.; Martín, N. *Energy Environ. Sci.* **2011**, *4*, 765.

(18) Ventura, B.; Barbieri, A.; Zanelli, A.; Barigelletti, F.; Seneclauze, J. B.; Diring, S.; Ziessel, R. *Inorg. Chem.* **2009**, *48*, 6409.

(19) Liu, Y. F.; Zhao, J. Z. *Chem. Commun.* **2012**, *48*, 3751.

(20) Martín, N.; Sánchez, L.; Illescas, B.; Pérez, I. *Chem. Rev.* **1998**, *98*, 2527.

(21) Armaroli, N. *Photochem. Photobiol. Sci.* **2003**, *2*, 73.

(22) Medlycott, E. A.; Hanan, G. S. *Chem. Soc. Rev.* **2005**, *34*, 133.

(23) Medlycott, E. A.; Hanan, G. S. *Coord. Chem. Rev.* **2006**, *250*, 1763.

(24) *Photochemistry and Photophysics of Coordination Compounds I* ; Balzani, V., Campagna, S., Eds.; Springer: Berlin/Heidelberg, 2007.

DOI: 10.1021/ic502431x
Inorg. Chem. 2015, 54, 3159−3171

(25) Armaroli, N.; Accorsi, G.; Felder, D.; Nierengarten, J. F. *Chem. Eur. J.* **2002**, *8*, 2314.
(26) Chaignon, F.; Torroba, J.; Blart, E.; Borgström, M.; Hammarström, L.; Odobel, F. *New J. Chem.* **2005**, *29*, 1272.
(27) Zhou, Z. G.; Sarova, G. H.; Zhang, S.; Ou, Z. P.; Tat, F. T.; Kadish, K. M.; Echegoyen, L.; Guldi, D. M.; Schuster, D. I.; Wilson, S. R. *Chem. Eur. J.* **2006**, *12*, 4241.
(28) Maggini, M.; Guldi, D. M.; Mondini, S.; Scorrano, G.; Paolucci, F.; Ceroni, P.; Roffia, S. *Chem. Eur. J.* **1998**, *4*, 1992.
(29) Allen, B. D.; Benniston, A. C.; Harriman, A.; Mallon, L. J.; Pariani, C. *Phys. Chem. Chem. Phys.* **2006**, *8*, 4112.
(30) Karlsson, S.; Modin, J.; Becker, H. C.; Hammarström, L.; Grennberg, H. *Inorg. Chem.* **2008**, *47*, 7286.
(31) Armaroli, N.; Barigelletti, F.; Ceroni, P.; Eckert, J. F.; Nicoud, J. F.; Nierengarten, J. F. *Chem. Commun.* **2000**, 599.
(32) Sariciftci, N. S.; Wudl, F.; Heeger, A. J.; Maggini, M.; Scorrano, G.; Prato, M.; Bourassa, J.; Ford, P. C. *Chem. Phys. Lett.* **1995**, *247*, 510.
(33) Armspach, D.; Constable, E. C.; Diederich, F.; Housecroft, C. E.; Nierengarten, J. F. *Chem.—Eur. J.* **1998**, *4*, 723.
(34) Polese, A.; Mondini, S.; Bianco, A.; Toniolo, C.; Scorrano, G.; Guldi, D. M.; Maggini, M. *J. Am. Chem. Soc.* **1999**, *121*, 3446.
(35) Albinsson, B.; Mårtensson, J. *J. Photochem. Photobiol., C* **2008**, *9*, 138.
(36) Siebert, R.; Winter, A.; Dietzek, B.; Schubert, U. S.; Popp, J. *Macromol. Rapid Commun.* **2010**, *31*, 883.
(37) Siebert, R.; Winter, A.; Schubert, U. S.; Dietzek, B.; Popp, J. *J. Phys. Chem. C* **2010**, *114*, 6841.
(38) Siebert, R.; Hunger, C.; Guthmuller, J.; Schlutter, F.; Winter, A.; Schubert, U. S.; González, L.; Dietzek, B.; Popp, J. *J. Phys. Chem. C* **2011**, *115*, 12677.
(39) Siebert, R.; Winter, A.; Schubert, U. S.; Dietzek, B.; Popp, J. *Phys. Chem. Chem. Phys.* **2011**, *13*, 1606.
(40) La Rosa, A.; Gillemot, K.; Leary, E.; Evangeli, C.; González, M. T.; Filippone, S.; Rubio-Bollinger, G.; Agraït, N.; Lambert, C. J.; Martín, N. *J. Org. Chem.* **2014**, *79*, 4871.
(41) Denholm, A. A.; George, M. H.; Hailes, H. C.; Tiffin, P. J.; Widdowson, D. A. *J. Chem. Soc., Perkin Trans. 1* **1995**, 541.
(42) Cave, G. W. V.; Raston, C. L. *J. Chem. Soc., Perkin Trans. 1* **2001**, 3258.
(43) Egbe, D. A. M.; Carbonnier, B.; Ding, L. M.; Mühlbacher, D.; Birckner, E.; Pakula, T.; Karasz, F. E.; Grummt, U. W. *Macromolecules* **2004**, *37*, 7451.
(44) Schlütter, F.; Wild, A.; Winter, A.; Hager, M. D.; Baumgärtel, A.; Friebe, C.; Schubert, U. S. *Macromolecules* **2010**, *43*, 2759.
(45) Hirsch, A. *Synthesis* **1995**, 895.
(46) Yamada, M.; Akasaka, T.; Nagase, S. *Chem. Rev.* **2013**, *113*, 7209.
(47) Winter, A.; Egbe, D. A. M.; Schubert, U. S. *Org. Lett.* **2007**, *9*, 2345.
(48) Winter, A.; Friebe, C.; Hager, M. D.; Schubert, U. S. *Eur. J. Org. Chem.* **2009**, 801.
(49) Maggini, M.; Donò, A.; Scorrano, G.; Prato, M. *J. Chem. Soc., Chem. Commun.* **1995**, 845.
(50) Schulze, B.; Escudero, D.; Friebe, C.; Siebert, R.; Görls, H.; Sinn, S.; Thomas, M.; Mai, S.; Popp, J.; Dietzek, B.; González, L.; Schubert, U. S. *Chem. - Eur. J.* **2012**, *18*, 4010.
(51) Sinn, S.; Schulze, B.; Friebe, C.; Brown, D. G.; Jäger, M.; Kübel, J.; Dietzek, B.; Berlinguette, C. P.; Schubert, U. S. *Inorg. Chem.* **2014**, *53*, 1637.
(52) Barigelletti, F.; Flamigni, L.; Balzani, V.; Collin, J. P.; Sauvage, J. P.; Sour, A.; Constable, E. C.; Cargill Thompson, A. M. W. *J. Am. Chem. Soc.* **1994**, *116*, 7692.
(53) Lukoyanova, O.; Cardona, C. M.; Altable, M.; Filippone, S.; Martín Domenech, Á.; Martín, N.; Echegoyen, L. *Angew. Chem., Int. Ed.* **2006**, *45*, 7430.
(54) Hirsch, A.; Brettreich, M. *Fullerenes*; Wiley-VCH: Weinheim, Germany, 2005.
(55) Herranz, M. Á.; Diederich, F.; Echegoyen, L. *Eur. J. Org. Chem.* **2004**, 2299.
(56) Schubert, U. S.; Winter, A.; Newkome, G. R. *Terpyridine-based Materials*; Wiley-VCH: Weinheim, Germany, 2011.
(57) Thomas, K. G.; Biju, V.; Guldi, D. M.; Kamat, P. V.; George, M. V. *J. Phys. Chem. B* **1999**, *103*, 8864.
(58) Bensasson, R. V.; Bienvenüe, E.; Fabre, C.; Janot, J. M.; Land, E. J.; Leach, S.; Leboulaire, V.; Rassat, A.; Roux, S.; Seta, P. *Chem. Eur. J.* **1998**, *4*, 270.
(59) Amouyal, E.; Mouallem-Bahout, M.; Calzaferri, G. *J. Phys. Chem.* **1991**, *95*, 7641.
(60) Horng, M. L.; Gardecki, J. A.; Papazyan, A.; Maroncelli, M. *J. Phys. Chem.* **1995**, *99*, 17311.
(61) Bhasikuttan, A. C.; Suzuki, M.; Nakashima, S.; Okada, T. *J. Am. Chem. Soc.* **2002**, *124*, 8398.
(62) Maestri, M.; Armaroli, N.; Balzani, V.; Constable, E. C.; Cargill Thompson, A. M. W. *Inorg. Chem.* **1995**, *34*, 2759.
(63) Lainé, P. P.; Campagna, S.; Loiseau, F. *Coord. Chem. Rev.* **2008**, *252*, 2552.
(64) McClenaghan, N. D.; Leydet, Y.; Maubert, B.; Indelli, M. T.; Campagna, S. *Coord. Chem. Rev.* **2005**, *249*, 1336.
(65) Grewer, C.; Brauer, H.-D. *J. Phys. Chem.* **1994**, *98*, 4230.
(66) Winter, A.; van den Berg, A. M. J.; Hoogenboom, R.; Kickelbick, G.; Schubert, U. S. *Synthesis* **2006**, 2873.
(67) Sullivan, B. P.; Calvert, J. M.; Meyer, T. J. *Inorg. Chem.* **1980**, *19*, 1404.
(68) Igartúa-Nieves, E.; Ocasio-Delgado, Y.; Torres-Castillo, M. D. L. A.; Rivera-Betancourt, O.; Rivera-Pagán, J. A.; Rodriguez, D.; López, G. E.; Cortés-Figueroa, J. E. *Dalton Trans.* **2007**, 1293.

DOI: 10.1021/ic502431x
Inorg. Chem. 2015, 54, 3159−3171